Bioorganic & Medicinal Chemistry 20 (2012) 6465–6481

Contents lists available at SciVerse ScienceDirect

Bioorganic & Medicinal Chemistry

journal homepage: www.elsevier.com/locate/bmc

Potent small molecule Hedgehog agonists induce VEGF expression in vitro

Katrin Seifert [a,†], Anita Büttner [a,†], Stephan Rigol [a], Nicole Eilert [a], Elke Wandel [b], Athanassios Giannis [a,*]

[a] Universität Leipzig, Fakultät für Chemie und Mineralogie, Institut für Organische Chemie, Johannisallee 29, 04103 Leipzig, Germany
[b] TRM-Leipzig/Research laboratories, Department of Surgery, Liebigstraße 20, 04103 Leipzig, Germany

ARTICLE INFO

Article history:
Received 27 June 2012
Revised 17 August 2012
Accepted 20 August 2012
Available online 28 August 2012

Keywords:
Hedgehog
SAG
VEGF

ABSTRACT

Here, we describe the synthesis, SAR studies as well as biological investigations of the known Hedgehog signaling agonist SAG and a small library of its analogues. The SAG and its derivatives were analyzed for their potency to activate the expression of the Hh target gene *Gli1* in a reporter gene assay. By analyzing SAR important molecular descriptors for *Gli1* activation have been identified. SAG as well as compound **10c** proven to be potent activators of VEGF expression in cultivated dermal fibroblasts. Importantly and in contrast to SAG, derivative **10c** displayed no toxicity in concentrations up to 250 μm.

1. Introduction

Hedgehog proteins are morphogens that act in a wide variety of tissues during embryonic development[1] and also in adult homeostatic processes, such as tissue maintenance and regeneration.[2,3] In mammals, three Hh proteins were identified: Sonic (Shh), Indian (Ihh) and Desert (Dhh) Hedgehog. The Hh precursor proteins are autocatalytically cleaved, resulting in active amino peptides, which are modified by the addition of a cholesterol moiety at the C-terminal amino acid glycine and a palmitoyl group at the N-terminal amino acid cysteine, respectively.[4] Mammalian Hh signaling occurs through the interaction of secreted Hh proteins with the 12-pass transmembrane receptors Patched-1 (Ptch1) and Patched-2 (Ptch2) which in turn inactivate the repression of the 7-pass transmembrane receptor Smoothened (Smo). After binding of Hh to Ptch the receptor-ligand-complex gets internalized, while Smo is phosphorylated[5] and translocated from the primarily cytoplasmic localization to the tip of the cilium, probably through an intraflagellar transport (IFT) pathway, resulting in a transcription factor Gli (*Gli1*/*Gli2*)-mediated activation of transcriptional targets of the Hh pathway.[6]

Hedgehog signaling plays not only a key role in vertebrate organogenesis[7], it is also crucial for postnatal tissue repair and vascular development.[8,9] It has been shown that Shh is a potent angiogenic agent in vivo and has an indirect role in angiogenesis by acting upstream of angiogenic factors. In a hind limb ischemia model Shh treatment promoted new vessel growth, characterized by distinct large-diameter vessels, and an increase in blood flow.[10] In vitro, Shh was not able to promote cell migration or proliferation of endothelial cells, instead it was able to induce capillary morphogenesis[11] by human umbilical endothelial cells as well as by murine brain capillary endothelial cells. In this study, the Sonic Hedgehog protein increased Phosphoinositide 3-Kinase (PI3-kinase) activity, an enzyme whose down-stream signaling might be linked to the inhibition of Gli degradation and thus to the expression of Hh target genes. Moreover, Asai et al.[12] showed that dermal fibroblasts can be activated in vitro by exogenous Shh stimulation, resulting in expression of several angiogenic cytokines (VEGF, Ang-1, Ang-2) and induction of proliferative activity. From pre-clinical studies it is known that angiogenic growth factors, such as VEGF, FGF-1, FGF-2, and angiopoietin-related growth factor (AGF) can promote vessel growth in vivo and microvascular endothelial cell morphogenesis in vitro.[13] Recently, it was published that Hedgehog proteins activate pro-angiogenic responses in endothelial cells through a new Gli-independent non-canonical Hedgehog signaling pathway.[14] Hence, Hedgehog signaling represents a key element in ischemia-induced angiogenesis. The connection between Hedgehog signaling pathway and vascular development remains still elusive and its understanding represents a promising challenge for the development of future therapies for severe tissue ischemia diseases. However, the use of topical Shh protein in vivo is limited due to rapid protein degradation. Therefore, proteolytically stable molecules with similar biological properties like Shh would be of high value. Several non-peptidic small molecule activators[15,16] of the Hh pathway are known, although no investigations concerning their angiogenic activity have been reported yet. Thus, we intended to shade more lights into the mode of action of the well-known small molecule agonist SAG.[15]

* Corresponding author. Fax: +49 341 9736599.
E-mail address: giannis@uni-leipzig.de (A. Giannis).
† These authors contributed equally to this work.

0968-0896/$ - see front matter © 2012 Elsevier Ltd. All rights reserved.
http://dx.doi.org/10.1016/j.bmc.2012.08.026

The aim of this study was to establish an efficient and diversity-oriented synthesis route to SAG and its analogues in order to evaluate their potential activating effects on the Hedgehog signaling pathway. Furthermore, we performed SAR studies using these analogues. Shh activation was measured by analyzing the expression of the Hedgehog signaling target gene *Gli1* using a reporter gene assay. Finally, we tested these small molecule agonists for their angiogenic activity. Since Shh is known to induce the expression of angiogenic factors by fibroblasts in vitro, we treated human primary fibroblasts with different compound concentrations and determined VEGF expression. Additionally, we used endothelial cells for analyzing cytotoxic effects of the active compounds.

2. Results and discussion

2.1. Synthesis of SAG and analogues

In 2002 Beachy and co-workers published the synthesis of SAG.[15] However, the key intermediate **1a** was synthesized in five steps and could only be obtained in 11% overall yield. Besides this Ducruet et al. published a synthesis route of the not methylated derivative **2** with a yield of only 21% (Fig. 1).[17,18]

We were able to establish an efficient synthesis route to access the key intermediate **1a** and its *cis* analogue **1b** in very good yields and purity. As highlighted in Scheme 1, commercially available *trans*-4-aminocyclohexanol **3** was Boc-protected at the amino-terminus supported by ultrasound, the yielded carbamate then was reduced with $LiAlH_4$ to furnish the corresponding methylamine and in a final step Boc-protected using sonication to give carbamate **4**.

Mitsunobu reaction and substitution of the hydroxyl group afforded azidocarbamate **6**, which was finally reduced to the desired key intermediate **1a** in 86% overall yield. The *cis* analogue **1b** was obtained in 80% overall yield using a similar approach of substitution and reduction. With these key intermediates in our hands we were able to synthesize SAG (**10a**) and its 1,4-diaminocyclohexane analogues (**10b**–**10m** and **18**) by the following synthetic strategy: (i) reductive amination, (ii) acylation and (iii) deprotection (Scheme 2). Additionally, piperidine derivatives (**14a**–**14q**) were prepared in a similar way as depicted in Scheme 3. The Boc-protected *trans*-aminopiperidine **11** was formed by in situ protection of the primary amino group with benzaldehyde (for reaction scheme see Supplementary data). Suzuki coupling reaction of 4-brompyridine hydrochloride **15** and 3-formylphenylboronic acid **16** yielded 3-pyridinylbenzaldehyde **17** (Scheme 4). The other aldehydes used were commercially available. The carboxylic chlorides were either commercially available or prepared from the corresponding acids.

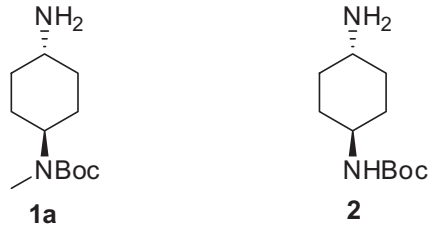

Figure 1. Key intermediates for synthesis of SAG.

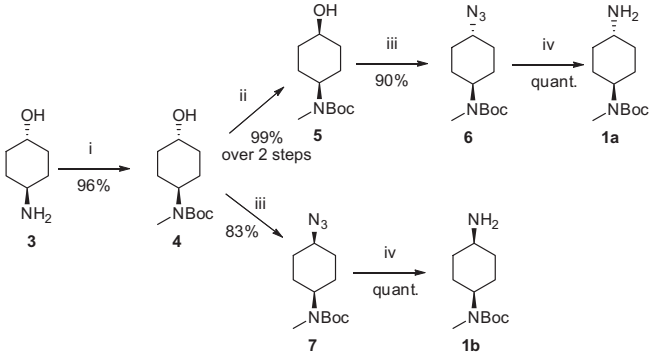

Scheme 1. Reagents and conditions: (i) (a) Boc_2O, THF, rt, 1.25 h,))); (b) $LiAlH_4$, THF, 0 °C → reflux, 6 h; (c) Boc_2O, THF, rt, 3 h,))); (ii) (a) PPh_3, BzOH, DEAD, toluene, −30 °C → 0 °C → rt, 14.5 h; (b) NaOMe in MeOH (1 m), THF, rt, 20 h; (iii) (a) CH_3SO_2Cl, NEt_3, CH_2Cl_2, 0 °C → rt, 3.5 h; (b) NaN_3, DMF, 85 °C, 12 h; (iv) Pd/C, H_2, MeOH, rt → 40 °C, 1.5 h–4 h.

We were able to develop an efficient and diversity-oriented approach to a substance library of SAG analogues, which were analyzed relating to Shh pathway activation and used for SAR study.

2.2. Activation of *Gli1* reporter gene expression and SAR study

The structure of SAG (**10a**) can be divided into three parts, which are suitable for structural modification as indicated in Figure 2: the 1,4-diaminocyclohexane ring, the biaryl moiety, and the 3-chlorobenzo[*b*]thiophene group.

The synthesized compounds were tested for their interference with the Shh signaling pathway by an established reporter gene assay based on the activation of the target gene *Gli1*. The EC_{50}-values and their corresponding confidence intervals for activation of the *Gli1* reporter gene were determined (Table 1, Fig. 3 and Fig. 4). Compounds with non-overlapping confidence intervals were considered to exhibit significantly different EC_{50}-values. According to the results of these studies the derivatives were classified into four distinct groups (Fig. 5A–D).

The first group (Fig. 5A) consists of the most potent agonists with similar EC_{50}-values as the parent compound SAG. The second group (Fig. 5B) had approximately sevenfold higher EC_{50}-values. About 13-fold higher EC_{50}-values were determined for group 3 (Fig. 5C). Group 4 summarizes compounds with no activity in the range up to 1 μm (Fig. 5D).

Gli1 expression was measured in Shh-light II cells. EC_{50}-values were calculated from three replicated independent experiments. Highest tested concentration of each compound = 1000 nm. Compounds **10h**–**10m** and **14a**–**14r** did not provoke any stimulation of *Gli1* expression.

Structural modifications will be discussed in the following order: SAR at the 1,4-diaminocyclohexane ring, SAR referring to the biaryl group, and SAR at the 3-chlorobenzo[*b*]thiophene group.

The replacement of the 1,4-diaminocyclohexane ring of SAG (**10a**) with a piperidine ring (**14a**) resulted in complete loss of Shh activity independently from any other modifications of the two remaining variable moieties. An extended series of further not active piperidine derivatives (**14b**–**14r**, Fig. 5D1, Supplementary data) affirm the importance of the 1,4-diaminocyclohexane ring.

Modification of the relative configuration of the 1,4-diaminocyclohexane ring led to interesting results. We observed an eightfold activity loss of the *cis* analogue **10e** compared to its *trans* derivative **10a**. In contrast, the *cis* derivative **10b** increased the activity compared to its *trans* analogue **10c** and showed similar potency as the parent compound SAG **10a**. Hence, the influence of the relative configuration of the 1,4-diaminocyclohexane ring remains unclear.

In agreement with other previous studies[19–21] our results confirmed the crucial dependence on the biaryl scaffold, since a replacement of the biaryl group with quinoline (**10l**) and pyridine (**10m**), respectively, led to loss of activity in the range up to 1 μm.

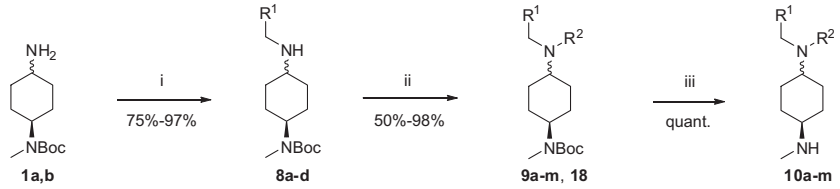

	R¹		R¹	R²
1a *trans*	8a *trans*	3-pyridin-4-ylphenyl	9a, 10a *trans* 3-pyridin-4-ylphenyl	(3-chlorobenzo[*b*]thiophen-2-yl) carbonyl
1b *cis*	8b *cis*	3-pyridin-4-ylphenyl	9b, 10b *cis* 3-pyridin-4-ylphenyl	(3,4-dichlorobenzo[*b*]thiophen-2-yl)carbonyl
	8c *trans*	quinolin-4-yl	9c, 10c *trans* 3-pyridin-4-ylphenyl	(3,4-dichlorobenzo[*b*]thiophen-2-yl)carbonyl
	8d *trans*	pyridin-4-yl	9d, 10d *trans* 3-pyridin-4-ylphenyl	(5-phenylfuran-2-yl)carbonyl
			9e, 10e *cis* 3-pyridin-4-ylphenyl	(3-chlorobenzo[*b*]thiophen-2-yl)carbonyl
			9f, 10f *trans* 3-pyridin-4-ylphenyl	(3-chloro-1*H*-indol-2-yl)carbonyl
			9g, 10g *trans* 3-pyridin-4-ylphenyl	(3-chloro-6-fluorobenzo[*b*]thiophen-2-yl) carbonyl
			9h, 10h *trans* 3-pyridin-4-ylphenyl	(3,6-dichlorobenzo[*b*]thiophen-2-yl)carbonyl
			9i, 10i *trans* 3-pyridin-4-ylphenyl	(benzo[*b*]thiophen-2-yl)carbonyl
			9j, 10j *trans* 3-pyridin-4-ylphenyl	(3-methylbenzo[*b*]furan-2-yl) carbonyl
			9k, 10k *trans* 3-pyridin-4-ylphenyl	(3,4,5-triethoxybenzoyl)carbonyl
			9l, 10l *trans* quinolin-4-yl	(3-chlorobenzo[*b*]thiophen-2-yl)carbonyl
			9m, 10m *trans* pyridin-4-yl	(3-chlorobenzo[*b*]thiophen-2-yl)carbonyl
			18 *trans* 3-pyridin-4-ylphenyl	H

Scheme 2. Reagents and conditions: (i) aldehyde, $MgSO_4$, $NaBH_4$, EtOH, 70 °C → rt, 22 h; (ii) acid chloride, NEt_3, DMAP, CH_2Cl_2, rt, 16 h; **9f** was prepared using 3-chloro-1*H*-indole carboxylic acid, PyBob, NEt_3, DMF, rt, 36 h; (iii) CF_3COOH, CH_2Cl_2, rt, 30 min–5 h; **18** was prepared directly from **8a** through treatment with TFA.

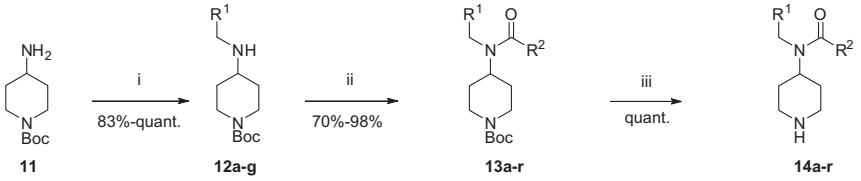

	R¹		R¹		R²
12a	3-pyridin-4-ylphenyl	13a, 14a	3-pyridin-4-ylphenyl	3-chlorobenzo[*b*]thiophen-2-yl
12b	quinolin-4-yl	13b, 14b	3-pyridin-4-ylphenyl	3,4-dichlorobenzo[*b*]thiophen-2-yl
12c	3-bromophenyl	13c, 14c	3-pyridin-4-ylphenyl	3-chloro-6-fluorobenzo[*b*]thiophen-2-yl
12d	4-(acetylamino)phenyl	13d, 14d	quinolin-4-yl	3-chlorobenzo[*b*]thiophen-2-yl
12e	4-cyanophenyl	13e, 14e	3-bromophenyl	3-chlorobenzo[*b*]thiophen-2-yl
12f	furan-2-yl	13f, 14f	4-(acetylamino)phenyl	3-chlorobenzo[*b*]thiophen-2-yl
12g	thiophen-2-yl	13g, 14g	4-(acetylamino)phenyl	3,4-dichlorobenzo[*b*]thiophen-2-yl
		13h, 14h	4-(acetylamino)phenyl	3-chloro-6-fluorobenzo[*b*] thiophen-2-yl
		13i, 14i	4-(acetylamino)phenyl	3-methylbenzo[*b*]furan-2-yl
		13j, 14j	4-cyanophenyl	3-chlorobenzo[*b*]thiophen-2-yl
		13k, 14k	4-cyanophenyl	3,4-dichlorobenzo[*b*]thiophen-2-yl
		13l, 14l	4-cyanophenyl	3-chloro-6-fluorobenzo[*b*] thiophen-2-yl
		13m, 14m	furan-2-yl	3-chlorobenzo[*b*]thiophen-2-yl
		13n, 14n	furan-2-yl	3,4-dichlorobenzo[*b*]thiophen-2-yl
		13o, 14o	furan-2-yl	3-chloro-6-fluorobenzo[*b*] thiophen-2-yl
		13p, 14p	furan-2-yl	3-methylbenzo[*b*]furan-2-yl
		13q, 14q	thiophen-2-yl	3-chlorobenzo[*b*]thiophen-2-yl
		13r, 14r	thiophen-2-yl	3-methylbenzo[*b*]furan-2-yl

Scheme 3. Reagents and conditions: (i) aldehyde, $MgSO_4$, $NaBH_4$, EtOH, 70 °C → rt, 22 h; (ii) acid chloride, NEt_3, DMAP, CH_2Cl_2, rt, 16 h; (iii) CF_3COOH, CH_2Cl_2, rt, 30 min–5 h.

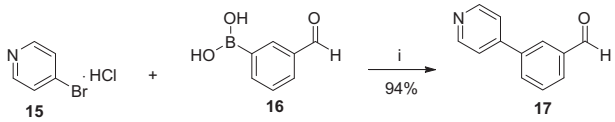

Scheme 4. Reagents and conditions: (i) $Pd(PPh_3)_4$, Na_2CO_3, toluene/H_2O (1:2), 0 °C → 85 °C, 18 h.

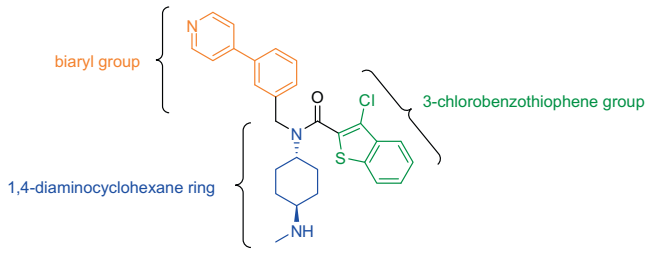

Figure 2. The three parts of the known Hedgehog agonist SAG.

Finally, the influence of halogen substitutions in the 3-chlorobenzo[*b*]thiophene group as well as the importance of the benzothiophene moiety itself was explored. Removal (see **18**) and replacement of the 3-chlorobenzo[*b*]thiophenecarboxamide group with triethoxybenzoyl or 3-methylbenzofuranyl resulted in loss of activity (see **10k**, **10j**). Also the removal of the chlorine substituent in the 3-position of the benzothiophene group led to an inactive compound (**10i**). According to these results it seems that the 3-chlorobenzo[*b*]thiophene moiety is of importance for Shh activation. However, also compounds **10d** and **10f** showed an agonistic

Table 1
EC_{50}-values, slope (p) of non-linear regression curves (Hill-slope equation), corresponding standard errors (SE) and confidence intervals for the activation of *Gli1* reporter gene expression in Shh-Light II cells by SAG and its derivatives (see also Figs. 3 and 5 for graphical representation and compound structures)

Compound	EC_{50} (nm)	SE	Confidence interval		Slope (p)	SE
			Lower level	Upper level		
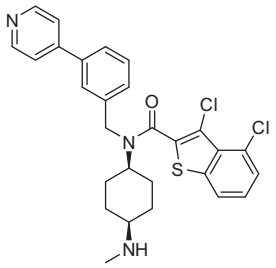 **10b**	7.6	1.2	5.4	10.2	1.4	0.4
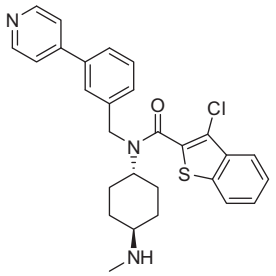 **10a**	8.8	1.4	6.4	12.6	1.4	0.4
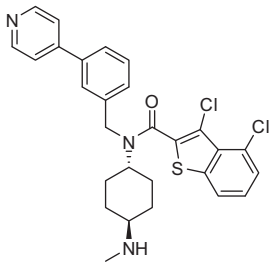 **10c**	21.9	4.8	13.8	34.3	0.8	0.1
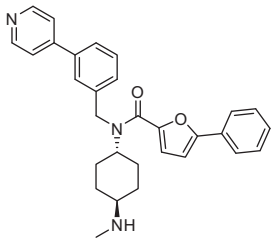 **10d**	53.8	6.7	40.3	67.8	2.0	0.5
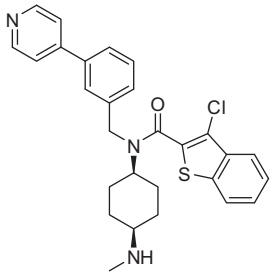 **10e**	61.8	5.8	50.6	75.1	0.9	0.1

Table 1 (*continued*)

Compound	EC_{50} (nm)	SE	Confidence interval		Slope (p)	SE
			Lower level	Upper level		
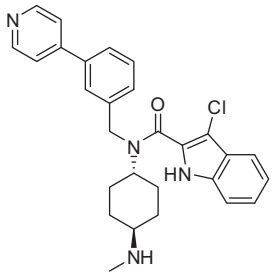 **10f**	117.8	28.7	65.1	192.8	1.2	0.3
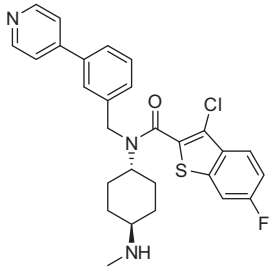 **10g**	175.6	9.8	156.4	197.3	2.0	0.1

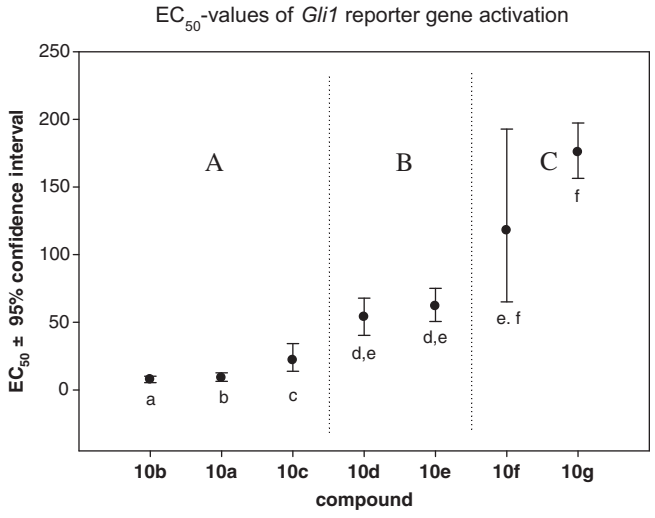

Figure 3. EC_{50}-values (in nm) for the activation of *Gli1* reporter gene expression in Shh-light II cells exposed to various concentrations of SAG and its derivatives. Data points represent EC_{50}-value ± upper and lower confidence intervals. Each compound was tested in three independent experiments. Letters indicate groups of compounds with no or slight overlapping confidence intervals.

activity, although they lack in the above-mentioned structural feature. The derivative **10d** posses a 5-phenylfuranyl moiety and compound **10f** is characterized by replacement of the sulphur atom with a NH-group, a proton-donating group. The Shh antagonist SANT-2, which binds to the smoothened receptor as well as SAG, is characterized by such a proton-donating group in its essential benzimidazole core.[22] In contrast, the sulphur atom in SAG represents a proton-accepting group. The compounds **10h**, **10g**, **10c** and **10b** vary in different substitution modes of chlorine and fluorine atoms in the 3-chlorobenzothiophene moiety. Surprisingly, replacement of hydrogen in 6-position with chlorine resulted in loss of activity (**10h**). However, insertion of chlorine in 4-position and fluorine in 6-position gave the potent analogues **10b** with an EC_{50} of ~7 nm, **10c** (EC_{50} ~22 nm) and **10g** (EC_{50} ~175 nm).

All six active compounds were analyzed regarding their cytotoxicity using HUVE cells. No toxic effect could be observed for a concentration up to 10 μm. Furthermore, analogue **10c** with an IC_{50} of ~250 μm has an approximately 10-fold lower toxicity than the parent compound SAG (IC_{50} ~22 μm, data not shown).

2.3. Shh agonists induce VEGF expression in vitro

We tested the hypothesis that Shh agonists might induce the production of the angiogenic cytokine VEGF in fibroblasts. Human primary fibroblasts of foreskin tissue were treated with the selected active compounds in a concentration range from 0.1 to 1.0 μm for 48 h and subsequently, the induction of VEGF protein was evaluated. ELISA detection showed that the primary fibroblasts responded to Shh agonists' stimulation by increased VEGF expression compared to vehicle-treated cells. Furthermore, the small molecule agonists induced VEGF expression in a concentration-dependent manner.

As shown in Figure 6, an up to sevenfold increase of VEGF concentration was determined for fibroblasts treated by the agonists **10a**, **10c**, **10e** and **10g**. For the parent compound SAG **10a** a maximum VEGF expression (29.61 ± 3.94 pg/ml) was obtained at a concentration of 0.5 μm. Compared to the other compounds the maximal VEGF concentration was detected at 1.0 μm (**10c**: 32.44 ± 4.41 pg/ml; **10e**: 23.83 ± 3.06 pg/ml and **10g**: 32.22 ± 4.42 pg/ml). A time dependence of VEGF expression as it was shown for Shh protein[10] could not be observed (data not shown).

In agreement with previous studies[10,12] the treatment of human umbilical vein endothelial cells (HUVECs) with the synthesized agonists did not lead to proliferation or formation of endothelial cell sprouts investigated by using 3D-angiogenesis and BrdU cell proliferation assay (data not shown).

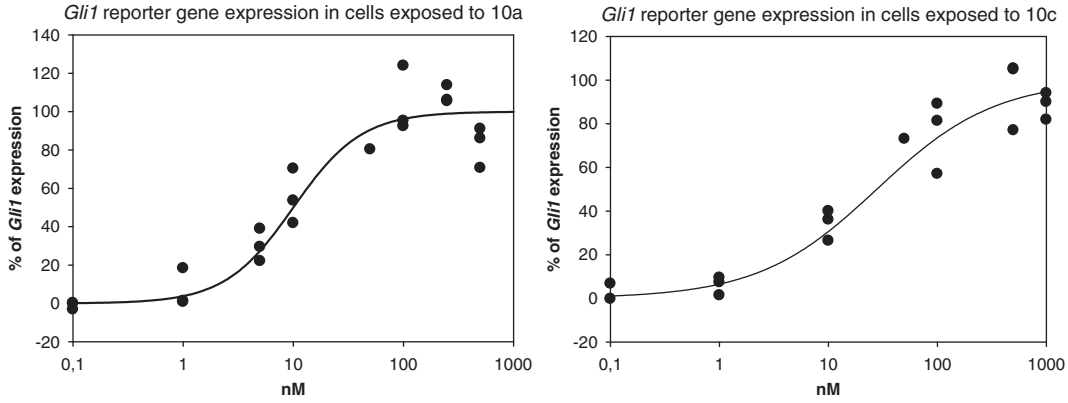

Figure 4. Examples of concentration-response curves for SAG (**10a**, *N* = 3) and its derivative **10c** (*N* = 3). Numbers refer to independent experiments.

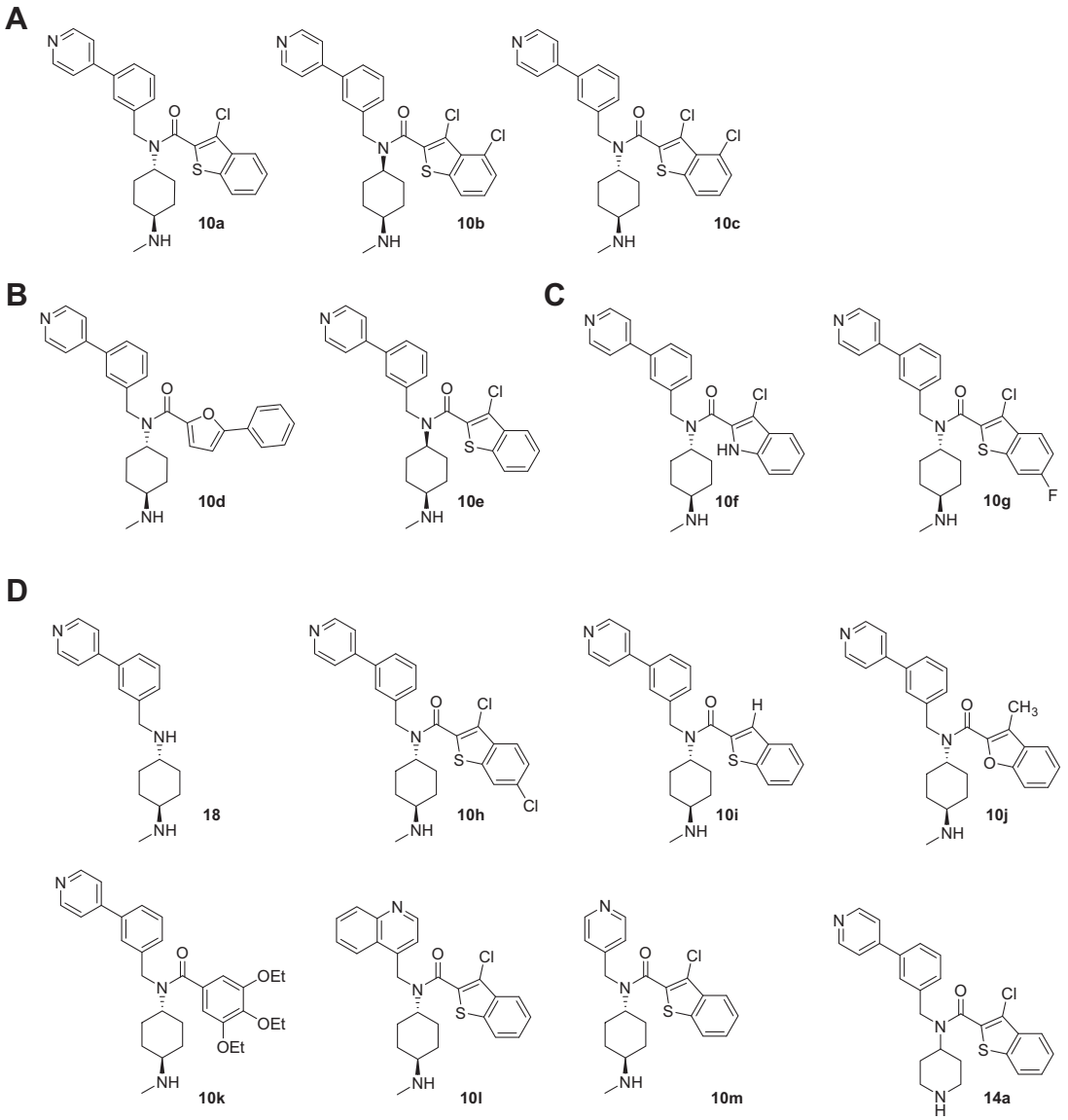

Figure 5. (A–D) structures of SAG derivatives classified according to their efficacy in activating *Gli1* reporter gene expression (see Fig. 5D1 in Supplementary data for structures of compounds **14b**–**14r**).

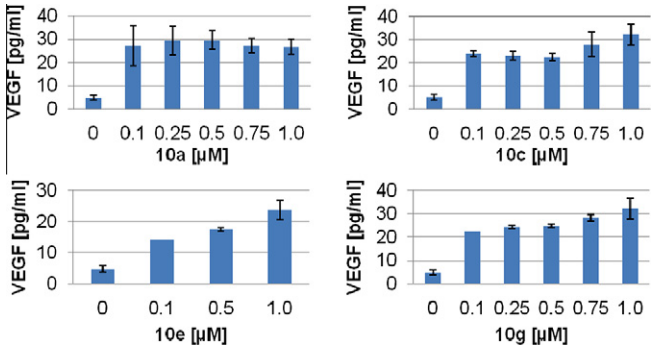

Figure 6. Induced VEGF expression in human primary foreskin fibroblasts treated by synthesized Shh agonists compared with vehicle-treated ones (0.1% DMSO) detected by ELISA after 48 h incubation.

Our results demonstrate that also small molecule Shh agonists are able to induce the production of the angiogenic growth factor VEGF in fibroblasts.

2.4. Conclusion

We have established an efficient approach to the key intermediates **1a** and **1b** leading to a synthesis for SAG and analogues. Additionally, our synthetic approach allows the investigation of SAR studies connected to the stereochemistry of the 1,4-diaminocyclohexane moiety since both diasteromers (**1a** and **1b**) are accessible. In summary, 31 SAG analogues could be synthesized. The results of our SAR study clearly demonstrate that both the 1,4-diaminocyclohexane and the biaryl scaffold are exquisitely important for the activation of the Hedgehog signaling pathway. Structural modifications of these two moieties led to inactive derivatives except changing the relative configuration of the 1,4-diaminocyclohexane ring. Because of the contrarian results of compounds **10b** and **10e** the influence of the relative configuration remains unclear and opens new possibilities for SAR studies. Structural modifications of the 3-chlorobenzothiophene moiety led to tiered active derivatives. However, the chlorine substituent in 3-position is also crucial for bioactivity. In conclusion, six new Shh agonists with nanomolar potency and no toxicity in the efficient range have been identified.

Previous reports have clearly shown that Shh has angiogenic activity in vivo and that dermal fibroblasts are activated in vitro by exogenous Shh stimulation, resulting in expression of several angiogenic cytokines (e.g. VEGF).[12] The mechanism by which Hh upregulates these angiogenic growth factors remains to be determined. In this context the non-canonical Hedgehog signaling should be taken into consideration.[14,23] Thus, no Gli response elements are present in the VEGF promoter region.[10] Our results give first evidence that also small molecule agonists can induce VEGF expression in primary dermal fibroblasts. A compound concentration of 0.5 μm already led to a significant increase of VEGF expression by fibroblasts. These data support the hypothesis that VEGF production from fibroblasts might amongst others be mediated by the Hh pathway. Furthermore, we suggest that also small molecule agonists of Hh signaling act as indirect angiogenic agents via upregulation of a subset of angiogenic cytokines in vivo. Thus, a small molecule agonist would represent an attractive alternative to Shh protein or gene therapy. We also investigated direct effects on endothelial cells. Neither proliferation nor migration in consequence of compound treatment could be observed. These findings are in agreement with previously reported results for the Sonic Hedgehog protein, indicating again a strong similarity in the mode of action of the protein and our small molecules.[10]

3. Experimental section

3.1. Chemistry

3.1.1. General

All materials were obtained from commercial suppliers and used without further purification. All reactions were performed under an argon atmosphere. Air- and moisture-sensitive chemicals were introduced via syringe or cannula through a rubber septum. Reactions were monitored by thin layer chromatography using Merck silica gel 60 F_{254} TLC aluminum sheets and visualized with UV light, ninhydrin and Seebach staining solution. Flash chromatography was performed on Merck silica gel 60. Melting points were determined on a Büchi Melting point B-540 apparatus and are uncorrected. IR data, recorded on FTIR spectrometer Genesis ATI (Mattson/Unicam), were determined for important intermediates and final compounds. ^{1}H, ^{13}C and ^{19}F NMR spectra were recorded on Varian Gemini 200BB, Varian Mercury plus 300 and Varian Mercury plus 400 NMR spectrometers at room temperature and at elevated temperature, respectively. High-resolution (HR) ESI mass spectra were obtained on Bruker Daltonics APEX II [7 T] FT-ICR mass spectrometer.

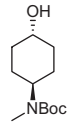

3.1.2. *tert*-Butyl (*trans*-4-hydroxycyclohexyl)methylcarbamate 4

A suspension of *trans*-4-aminocyclohexanol **3** (2.00 g, 17.4 mmol, 1.0 equiv) and di-*tert*-butyl dicarbonate (3.79 g, 17.4 mmol, 1.0 equiv) in dry THF (150 ml) was sonicated 1.25 h at rt. After removal of the solvent a beige residue was obtained.

To a suspension of lithium aluminium hydride (2.64 g, 69.5 mmol, 4.0 equiv) in dry THF (90 ml) was added slowly a solution of crude product in dry THF (60 ml) at 0 °C. The reaction mixture was stirred under reflux for 5 h. After cooling to 0 °C water (3.8 ml), 15 wt % sodium hydroxide solution (3.4 ml) and water (10 ml) were dropped subsequently and the resulting mixture was stirred at rt for 1 h. After filtration and washing with *tert*-butyl methyl ether (TBME, 2 × 75 ml) and CH_2Cl_2 (2 × 75 ml) the combined organic layers were dried over Na_2SO_4 and concentrated yielding the crude product as beige solid, which was used in the next step without further purification.

A suspension of crude product and di-*tert*-butyl dicarbonate (3.63 g, 16.6 mmol, 1.0 equiv) in dry THF (150 ml) was sonicated for 3 h. After removal of the solvent the residue was purified by column chromatography (CH_2Cl_2/MeOH 15:1 → 10:1, v/v) and gave **4** as a white solid (3.82 g, 96%); mp: 51–53 °C; IR (KBr): $\tilde{\nu}$ = 3445, 2940, 1664, 1367, 1321 cm^{-1}; ^{1}H NMR (400 MHz, $CDCl_3$): δ = 1.27–1.34 (m, 2H), 1.38 (s, 9H), 1.41–1.46 (m, 2H), 1.59–1.62 (m, 2H), 1.93–1.96 (m, 2H), 2.63 (s, 3H), 2.79 (br, 1H), 3.42–3.49 (m, 1H), 3.86 (br, 1H); ^{13}C NMR (100 MHz, $CDCl_3$): δ = 27.8, 28.3, 28.4, 34.5, 53.2 (br), 69.7, 79.4, 155.6; ESI-HRMS *m/z* calcd for $C_{12}H_{23}NO_3$: 252.15701 $[M+Na]^+$, 481.32481 $[2M+Na]^+$, found: 252.15703, 481.32491.

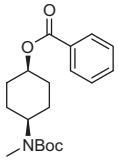

3.1.3. *cis*-4-[(*tert*-Butoxycarbonyl)(methyl)amino]cyclohexyl benzoate 19

Triphenylphosphine (2.75 g, 10.5 mmol, 1.2 equiv) and benzoic acid (1.28 g, 10.5 mmol, 1.2 equiv) were dissolved in dry toluene (30 ml) and cooled to −30 °C. A solution of *tert*-butyl (*trans*-4-hydroxycyclohexyl)methylcarbamate **4** (2.00 g, 8.72 mmol, 1.0 equiv) in dry toluene (6 ml) was added and then a solution of DEAD (1.82 g, 10.5 mmol, 1.2 equiv) in dry toluene (12 ml) was dropped slowly over a period of 15 min. The reaction was stirred at 0 °C for 2 h and then 12 h at rt. The reaction mixture was quenched with satd $NaHCO_3$ solution, extracted with EtOAc (3x50 ml) and the combined organic layers were dried over Na_2SO_4. After removal of the solvent the crude product was purified by column chromatography (*n*-hexane/EtOAc 4:1, v/v) to obtain **19** as colorless oil (2.88 g, 99%); IR (film): $\tilde{\nu}$ = 2939, 1717, 1692, 1378, 1277 cm^{-1}; ^1H NMR (400 MHz, $CDCl_3$): δ = 1.47 (s, 9H), 1.58–1.62 (m, 2H), 1.66–1.73 (m, 2H), 1.80–1.87 (m, 2H), 2.11–2.15 (m, 2H), 2.78 (s, 3H), 4.04 (br, 1H), 5.23–5.25 (m, 1H), 7.43–7.47 (m, 2H), 7.54–7.58 (m, 1H), 8.04–8.06 (m, 2H); ^{13}C NMR (100 MHz, $CDCl_3$): δ = 24.7, 28.4, 28.6, 29.7, 53.2 (br), 68.9, 79.5, 128.5, 129.6, 131.0, 133.0, 155.7, 165.8; ESI-HRMS *m/z* calcd for $C_{19}H_{27}NO_4$: 356.18323 $[M+Na]^+$, 689.37724 $[2M+Na]^+$, found: 356.18325, 689.37704.

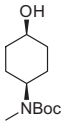

3.1.4. *tert*-Butyl (*cis*-4-hydroxycyclohexyl)methylcarbamate 5

To a solution of *cis*-4-[(*tert*-butoxycarbonyl)(methyl)amino]-cyclohexyl benzoate **19** (1.17 g, 3.52 mmol, 1.0 equiv) in dry THF (50 ml) was added a 1 m solution of NaOMe (1.89 g, 35.0 mmol, 10 equiv) in dry MeOH (35 ml) and stirred at rt for 20 h. After treatment with water (100 ml) and Et_2O (200 ml), the layers were separated and the aqueous layer was extracted with EtOAc (3 × 100 ml). The combined organic layers were dried over Na_2SO_4, concentrated and the obtained residue was purified by column chromatography (*n*-hexane/EtOAc 3:1 → 1:1, v/v) yielding **5** as colorless oil (804 mg, quantitative); IR (film): $\tilde{\nu}$ = 3439, 2933, 1668, 1384, 1151 cm^{-1}; ^1H NMR (400 MHz, $CDCl_3$): δ = 1.34–1.37 (m, 2H), 1.38 (s, 9H), 1.43–1.55 (m, 2H), 1.71–1.86 (m, 4H), 2.38 (br, 1H), 2.67 (s, 3H), 3.86 (br, 1H), 3.92–3.93 (m, 1H); ^{13}C NMR (100 MHz, $CDCl_3$): δ = 23.8, 28.5, 28.6, 32.3, 53.8 (br), 64.6, 79.4, 155.9; ESI-HRMS *m/z* calcd for $C_{12}H_{23}NO_3$: 252.15701 $[M+Na]^+$, 481.32481 $[2M+Na]^+$, found: 252.15700, 481.32482.

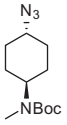

3.1.5. *tert*-Butyl (*trans*-4-azidocyclohexyl)methylcarbamate 6

To an ice-cooled solution of *tert*-butyl (*cis*-4-hydroxycyclohexyl)methylcarbamate **5** (189 mg, 0.824 mmol, 1.0 equiv) and NEt_3 (250 mg, 345 µl, 2.48 mmol, 3.0 equiv) in dry CH_2Cl_2 (8 ml) was added dropewise mesyl chloride (113 mg, 76.6 µl, 0.989 mmol, 1.2 equiv) and the solution was stirred at 0 °C for 15 min and additional 3 h at rt. After quenching with satd NH_4Cl solution (7 ml), the layers were separated and the aqueous layer was extracted with CH_2Cl_2 (3 × 25 ml). The combined organic layers were washed wit satd $NaHCO_3$ solution, dried over Na_2SO_4 and the solvent was removed under reduced pressure. The crude product was dissolved in dry DMF (8 ml) and sodium azide (64.4 mg, 0.989 mmol, 1.2 equiv) was added. After stirring at 85 °C for 12 h, water (10 ml) was added and the reaction mixture was extracted with CH_2Cl_2 (3 × 20 ml). The combined organic layers were dried over Na_2SO_4 and the solvent was removed under reduced pressure. The obtained residue was purified by column chromatography (*n*-hexane/EtOAc 50:1 → 10:1, v/v) to get **6** as a colorless oil (188 mg, 90%); IR (film): $\tilde{\nu}$ = 2936, 2864, 2094, 1691, 1367, 1150 cm^{-1}; ^1H NMR (300 MHz, $CDCl_3$): δ = 1.39–1.43 (m, 2H), 1.44 (s, 9H), 1.48–1.56 (m, 2H), 1.70–1.79 (m, 2H), 2.02–2.06 (m, 2H), 2.69 (s, 3H), 3.15–3.24 (m, 1H), 3.88 (br, 1H); ^{13}C NMR (75 MHz, $CDCl_3$): δ = 28.2, 28.5, 28.6, 31.0, 53.2 (br), 59.4, 79.6, 155.6; ESI-HRMS *m/z* calcd for $C_{12}H_{22}N_4O_2$: 277.16350 $[M+Na]^+$, 531.33777 $[2M+Na]^+$, found: 277.16362, 531.33752.

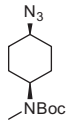

3.1.6. *tert*-Butyl (*cis*-4-azidocyclohexyl)methylcarbamate 7

To an ice-cooled solution of *tert*-butyl (*trans*-4-hydroxycyclohexyl)methylcarbamate **4** (130 mg, 0.567 mmol, 1.0 equiv) and NEt_3 (172 mg, 237 µl, 1.70 mmol, 3.0 equiv) in dry CH_2Cl_2 (5 ml) was added dropewise mesyl chloride (90.9 mg, 61.4 µl, 0.794 mmol, 1.4 equiv) and the solution was stirred at 0 °C for 15 min and additional 3 h at rt. After quenching with satd NH_4Cl solution (7 ml), the layers were separated and the aqueous layer was extracted with CH_2Cl_2 (3 × 25 ml). The combined organic layers were washed wit satd $NaHCO_3$ solution, dried over Na_2SO_4 and the solvent was removed under reduced pressure. The crude product was dissolved in dry DMF (5 ml) and sodium azide (51.6 mg, 0.794 mmol, 1.4 equiv) was added. After stirring at 85 °C for 12 h, water (10 ml) was added and the reaction mixture was extracted with CH_2Cl_2 (3 × 20 ml). The combined organic layers were dried over Na_2SO_4 and the solvent was removed under reduced pressure. The obtained residue was purified by column chromatography (*n*-hexane/EtOAc 30:1 → 10:1, v/v) to get **7** as a white solid (119 mg, 83%); mp: 70–71 °C; IR (KBr): $\tilde{\nu}$ = 2978, 2941, 2106, 1680, 1331 cm^{-1}; ^1H NMR (300 MHz, $CDCl_3$): δ = 1.45 (s, 9H), 1.47–1.53 (m, 2H), 1.58–1.66 (m, 2H), 1.66–1.78 (m, 2H), 1.88–1.98 (m, 2H), 2.73 (s, 3H), 3.81–3.85 (m, 1H), 3.90 (br, 1H); ^{13}C NMR (75 MHz, $CDCl_3$): δ = 24.4, 28.5, 28.6, 29.3, 53.2 (br), 56.5, 79.5, 155.7; ESI-HRMS *m/z* calcd for $C_{12}H_{22}N_4O_2$: 277.16350 $[M+Na]^+$, 531.33777 $[2M+Na]^+$, found: 277.16361, 531.33745.

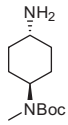

3.1.7. *tert*-Butyl (*trans*-4-aminocyclohexyl)methylcarbamate 1a

To a solution of *tert*-butyl (*trans*-4-azidocyclohexyl)methylcarbamate **6** (101 mg, 0.397 mmol, 1.0 equiv) in absolute MeOH (3 ml) was added palladium on charcoal (10% Pd) (10.1 mg, 10 mass %). The reaction mixture was stirred at 40 °C for 1.5 h under a hydrogen atmosphere. Then, the suspension was filtered over Celite® and the solvent was evaporated in vacuum yielding **1a** as a yellow oil (90.6 mg, quantitative); IR (film, CCl_4): $\tilde{\nu}$ = 2974, 2930, 2859, 1689, 1389, 1366, 1149 cm^{-1}; ^1H NMR (300 MHz, $CDCl_3$): δ = 1.20–1.25 (m, 2H), 1.43 (s, 9H), 1.44–1.53 (m, 2H), 1.60–1.69 (m, 2H), 1.82–1.92 (m, 2H), 2.52–2.64 (m, 1H), 2.68 (s, 3H), 3.87 (br, 1H); ^{13}C NMR (75 MHz, $CDCl_3$): δ = 28.4, 28.6, 28.7, 35.9, 50.2, 53.6 (br), 79.3, 155.8; ESI-HRMS *m/z* calcd for $C_{12}H_{24}N_2O_2$:

229.19105 $[M+H]^+$, 457.37483 $[2M+H]^+$, found: 229.19130, 457.37504.

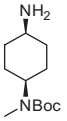

3.1.8. *tert*-Butyl (*cis*-4-aminocyclohexyl)methylcarbamate 1b

To a solution of *tert*-butyl (*cis*-4-azidocyclohexyl)-methylcarbamate **7** (2.80 g, 11.0 mmol, 1.0 equiv) in absolute MeOH (50 ml) was added palladium on charcoal (10% Pd) (280 mg, 10 mass %). The reaction mixture was stirred at rt for 4 h under a hydrogen atmosphere. Then, the suspension was filtered over Celite® and the solvent was evaporated in vacuum yielding **1b** as a colorless oil (2.51 g, quantitative); IR (film): $\tilde{\nu}$ = 3354, 2929, 1673, 1442, 1385, 1157 cm^{-1}; ^1H NMR (300 MHz, $CDCl_3$): δ = 1.25–1.37 (m, 2H), 1.45 (s, 9H), 1.59–1.68 (m, 4H), 1.71–1.85 (m, 2H), 2.75 (s, 3H), 3.15–3.19 (m, 1H), 3.85 (br, 1H); ^{13}C NMR (75 MHz, $CDCl_3$): δ = 23.7, 28.6, 32.6, 44.3, 54.4 (br), 79.3, 155.8; ESI-HRMS *m/z* calcd for $C_{12}H_{24}N_2O_2$: 229.19105 $[M+H]^+$, 457.37483 $[2M+H]^+$, found: 229.19125, 457.37480.

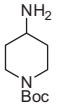

3.1.9. *tert*-Butyl 4-aminopiperidine-1-carboxylate 11

A solution of 4-aminopiperidine (5.00 g, 5.24 ml, 49.9 mmol, 1.0 equiv) and freshly distilled benzaldehyde (5.56 g, 5.30 ml, 52.4 mmol, 1.05 equiv) in toluene (50 ml) was heated to reflux for 5.5 h using a Dean-Stark apparatus. After cooling to 0 °C, di-*tert*-butyl dicarbonate (12.0 g, 54.9 mmol, 1.1 equiv) was added in portions over a period of 5 min and the reaction mixture was stirred at rt for 14 h. After removal of the solvent in vacuum the residue was suspended in 1 M $KHSO_4$ solution (167 ml), water (23 ml) and TBME (12 ml), and the mixture was stirred at rt for 4 h. Subsequently, TBME (70 ml) was added and the layers were separated. The aqueous layer was extracted with TBME (3 × 35 ml). Further, the aqueous layer was treated with 6 N NaOH solution to reach pH 13 and was extracted with CH_2Cl_2 (2 × 85 ml). The combined CH_2Cl_2-layers were washed with satd NaCl solution (2 × 60 ml) and were dried over Na_2SO_4. The solvent was removed under reduced pressure and the residue was purified by column chromatography (CH_2Cl_2/MeOH 50:1 → 10:1 + 1% *N*-ethyldimethylamine, v/v) to get **11** as yellow solid (6.0 g, 60%); mp: 66–67 °C; IR (film): $\tilde{\nu}$ = 2975, 2931, 1688, 1423, 1365, 1245, 1165, 769 cm^{-1} ; ^1H NMR (400 MHz, $CDCl_3$): δ = 1.17–1.21 (m, 2H), 1.34 (br, 2H), 1.41 (s, 9H), 1.72–1.76 (m, 2H), 2.71–2.75 (m, 2H), 2.76–2.80 (m, 1H), 3.98 (br, 2H); ^{13}C NMR (100 MHz, $CDCl_3$): δ = 28.5, 35.6, 42.7 (br), 48.9, 79.4, 154.9; ESI-HRMS *m/z* calcd for $C_{10}H_{20}N_2O_2$: 201.15975 $[M+H]^+$, 223.14170 $[M+Na]^+$, 401.31223 $[2\ M+H]^+$, 423.29418 $[2M+Na]^+$, found: 201.15984, 223.14183, 401.31195, 423.29414.

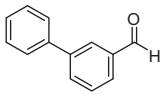

3.1.10. 3-Pyridin-4-ylbenzaldehyde 17

A mixture of 4-bromopyridine hydrochloride **15** (2.00 g, 10.3 mmol, 1.0 equiv) in water (16 ml) and toluene (22 ml) was cooled to 0 °C and a solution of Na_2CO_3 (2.51 g, 23.8 mmol, 2.3 equiv) in water (26 ml) was added. After warming to rt, 3-formylphenylboronic acid **16** (1.62 g, 10.8 mmol, 1.04 equiv) and $Pd(PPh_3)_4$ (0.600 g, 0.515 mmol, 0.05 equiv) were added and the reaction mixture was stirred at 85 °C for 18 h. Then, the cooled solution was diluted with CH_2Cl_2 (40 ml) and the layers were separated. The aqueous layer was extracted with CH_2Cl_2 (2 × 16 ml) and the combined organic layers were dried over $MgSO_4$. The solvent was removed under reduced pressure and the crude product was purified by column chromatography (*n*-hexane/EtOAc 4:1 → 1:4, v/v) to obtain **17** as a white solid (1.77 g, 94%); mp: 34–36 °C; IR (KBr): $\tilde{\nu}$ = 3440, 3025, 1689, 1582, 1379, 1188, 789, 690, 653 cm^{-1}; ^1H NMR (400 MHz, $CDCl_3$): δ = 7.51–7.53 (m, 2H), 7.63–7.67 (m, 1H), 7.87–7.94 (m, 2H), 8.12–8.13 (m, 1H), 8.68–8.70 (m, 2H), 10.08 (s, 1H); ^{13}C NMR (100 MHz, $CDCl_3$): δ = 121.7, 127.9, 130.0, 130.5, 132.9, 137.2, 139.3, 147.0, 150.6, 191.8; ESI-HRMS *m/z* calcd for $C_{12}H_9NO$: 206.05764 $[M+Na]^+$, 389.12605 $[2M+Na]^+$, found: 206.05779, 389.12615.

3.1.11. General procedure for preparing carbamates 8a, 8b, 8c, 8d and carboxylate 12a

Carbamate (1.0 equiv) or carboxylate (1.0 equiv), the corresponding aldehyde (1.0 equiv) and anhydrous $MgSO_4$ (1.5 equiv) were filled into a Pyrex® pressure flask, suspended in absolute EtOH and flushed with argon for 5 min. The mixture was heated to 80 °C for 8 h. After filtration of the cooled mixture, the filtrate was flushed again with argon and $NaBH_4$ (6.5 equiv) was added. The reaction was stirred at rt for 14 h (TLC control) and quenched with satd $NaHCO_3$ solution. After extraction with CH_2Cl_2 (three times) and washing with satd NaCl solution, the combined organic layers were dried over $MgSO_4$, concentrated and the obtained residue was purified by column chromatography using a sufficient mixture of CH_2Cl_2/MeOH (v/v) as eluent.

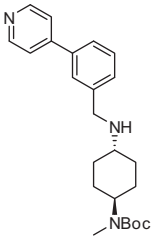

3.1.12. *tert*-Butyl methyl{*trans*-4-[(3-pyridin-4-ylbenzyl)amino]-cyclohexyl}carbamate 8a

Colorless oil, 97% yield. IR (film): $\tilde{\nu}$ = 2974, 2931, 1686, 1594, 1365, 1150, 788 cm^{-1}; ^1H NMR (400 MHz, $CDCl_3$): δ = 1.22–1.31 (m, 2H), 1.44 (s, 9H), 1.39–1.51 (m, 2H), 1.68–1.71 (m, 2H), 1.88 (br, 1H), 2.03–2.06 (m, 2H), 2.43–2.48 (m, 1H), 2.69 (s, 3H), 3.87 (s, 2H), 3.88 (br, 1H), 7.37–7.45 (m, 2H), 7.49–7.52 (m, 3H), 7.59 (s, 1H), 8.62–8.65 (m, 2H), ^{13}C NMR (100 MHz, $CDCl_3$): δ = 28.6, 32.5, 51.2, 53.9 (br), 55.9, 79.4, 121.8, 125.7, 126.8, 128.9, 129.3, 138.4, 141.6, 148.4, 150.3, 155.7; ESI-HRMS *m/z* calcd for $C_{24}H_{33}N_3O_2$: 396.26455 $[M+H]^+$, 791.52183 $[2M+H]^+$, found: 396.26487, 791.52188.

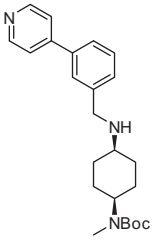

3.1.13. *tert*-Butyl methyl{*cis*-4-[(3-pyridin-4-ylbenzyl)amino]-cyclohexyl}carbamate 8b

Colorless oil, 75% yield. IR (film in CCl_4): $\tilde{\nu}$ = 3367, 2931, 2859, 1687, 1595, 1403, 1365, 1251 cm^{-1}; ^1H NMR (400 MHz, $CDCl_3$): δ = 1.22–1.42 (m, 4H), 1.44 (s, 9H), 1.65–1.75 (m, 2H), 1.85 (br, 1H), 2.01–2.10 (m, 2H), 2.43–2.54 (m, 1H), 2.69 (s, 3H), 3.89 (s, 2H), 3.95 (br, 1H), 7.38–7.46 (m, 2H), 7.49–7.53 (m, 3H), 7.62 (s, 1H), 8.63–8.65 (m, 2H); ^{13}C NMR (100 MHz, $CDCl_3$): δ = 28.6, 32.3, 51.0, 53.8 (br), 55.9, 79.4, 121.8, 125.9, 127.0, 129.0, 129.4, 138.5, 141.1, 148.3, 150.4, 155.7; ESI-HRMS *m/z* calcd for $C_{24}H_{33}N_3O_2$: 396.26455 $[M+H]^+$, 791.52183 $[2M+H]^+$, found: 396.26433, 791.52099.

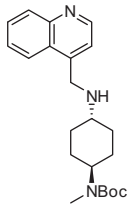

3.1.14. *tert*-Butyl methyl{*trans*-4-[(quinolin-4-ylmethyl)amino]-cyclohexyl}carbamate 8c

Colorless oil, 90% yield. ^1H NMR (300 MHz, $(CD_3)_2SO$, 90 °C): δ = 1.39 (s, 9H), 1.40–1.65 (m, 6H), 2.11–2.15 (m, 2H), 2.65 (s, 3H), 2.69–2.74 (m, 1H), 3.68–3.77 (m, 1H), 4.38 (s, 2H), 7.58–7.64 (m, 2H), 7.71–7.76 (m, 1H), 8.01–8.04 (m, 1H), 8.19–8.22 (m, 1H), 8.85 (d, *J* = 4.4 Hz, 1H); ^{13}C NMR (75 MHz, $(CD_3)_2SO$, 90 °C): δ = 27.5, 27.8, 28.0, 30.4, 45.2, 53.8, 55.7, 78.0, 120.2, 123.4, 126.0, 126.1, 128.7, 129.2, 143.5, 147.5, 149.7, 154.3; ESI-HRMS *m/z* calcd for $C_{22}H_{31}N_3O_2$: 370.24890 $[M+H]^+$, 392.23085 $[M+Na]^+$, found: 370.24891, 392.23080.

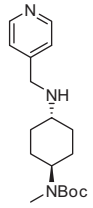

3.1.15. *tert*-Butyl methyl{*trans*-4-[(pyridin-4-ylmethyl)amino]-cyclohexyl}carbamate 8d

Yellow oil, 86% yield. ^1H NMR (300 MHz, $(CD_3)_2SO$, 90 °C): δ = 1.15–1.25 (m, 2H), 1.38 (s, 9H), 1.43–1.59 (m, 4H), 1.96–2.00 (m, 2H), 2.40–2.49 (m, 1H), 2.62 (s, 3H), 3.66–3.73 (m, 1H), 3.81 (s, 2H), 7.33–7.35 (m, 2H), 8.45–8.47 (m, 2H); ^{13}C NMR (75 MHz, $(CD_3)_2SO$, 90 °C): δ = 27.6, 27.8, 28.0, 31.1, 48.2, 53.9, 54.9, 78.0, 122.7, 148.7, 148.9, 154.3; ESI-HRMS *m/z* calcd for $C_{18}H_{29}N_3O_2$: 320.23320 $[M+H]^+$, 639.45923 $[2M+H]^+$, found: 320.23320, 639.45948.

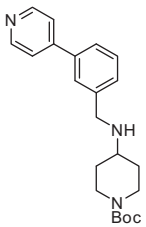

3.1.16. *tert*-Butyl 4-[(3-pyridin-4-ylbenzyl)amino]piperidine-1-carboxylate 12a

Colorless oil, 87% yield. IR (KBr): $\tilde{\nu}$ = 3317, 3274, 2974, 2928, 1678, 1594, 1427, 1170 cm^{-1}; ^1H NMR (300 MHz, $CDCl_3$): δ = 1.24–1.39 (m, 3H), 1.44 (s, 9H), 1.85–1.91 (m, 2H), 2.66–2.74 (m, 1H), 2.76–2.86 (m, 2H), 3.89 (s, 2H), 3.99–4.06 (m, 2H), 7.39–7.48 (m, 2H), 7.49–7.54 (m, 3H), 7.60 (s, 1H), 8.64 (br, 2H); ^{13}C NMR (100 MHz, $CDCl_3$): δ = 28.5, 32.6, 42.5 (br), 50.8, 54.6, 79.5, 121.8, 125.8, 126.8, 128.9, 129.3, 138.4, 141.6, 148.4, 150.3, 154.9; ESI-HRMS *m/z* calcd for $C_{22}H_{29}N_3O_2$: 368.23325 $[M+H]^+$, 390.21520 $[M+Na]^+$, 757.44118 $[2M+Na]^+$, found: 368.23308, 390.21493, 757.44138.

3.1.17. General procedure for preparing carbamates 9a, 9b, 9c, 9d, 9e, 9g, 9h, 9i, 9j, 9k, 9l, 9m and carboxylate 13a

To a solution of acyl chloride (1.0 equiv, commercially available or prepared from the corresponding acid) and *N*,*N*-dimethylpyridin-4-amine (0.1 equiv) in dry CH_2Cl_2 was added a solution of carbamate (1.0 equiv) or carboxylate (1.0 equiv) and NEt_3 (5.0 equiv) in dry CH_2Cl_2 at rt. The resulting solution was stirred at rt for 16 h (TLC control). The solvent was removed under reduced pressure and the crude product was purified by column chromatography using a sufficient mixture of *n*-hexane/acetone (v/v) as eluent.

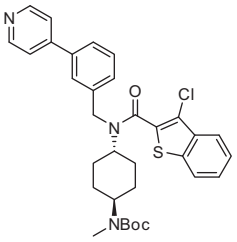

3.1.18. *tert*-Butyl (*trans*-4-{[(3-chlorobenzo[*b*]thiophene-2-yl)carbonyl](3-pyridin-4-yl benzyl)amino}cyclohexyl)-methylcarbamate 9a

White solid, 75% yield. Mp: 70–72 °C; IR (KBr): $\tilde{\nu}$ = 2932, 2862, 1686, 1636, 1441, 1365, 1147 cm^{-1}; ^1H NMR (300 MHz, $(CD_3)_2SO$, 90 °C): δ = 1.32 (s, 9H), 1.42–1.62 (m, 4H), 1.74–1.86 (m, 4H), 2.56 (s, 3H), 3.57–3.70 (m, 1H), 3.87 (br, 1H), 4.79 (s, 2H), 7.43–7.48 (m, 2H), 7.50–7.53 (m, 1H), 7.53–7.55 (m, 1H), 7.57–7.59 (m, 2H), 7.61–7.66 (m, 1H), 7.68 (br, 1H), 7.84–7.87 (m, 1H), 8.03–8.06 (m, 1H), 8.61–8.63 (m, 2H); ^{13}C NMR (75 MHz, $(CD_3)_2SO$, 90 °C): δ = 27.7, 27.9, 28.4, 29.3, 45.5 (br), 53.2, 58.1, 78.0, 117.2, 120.6, 121.5, 122.9, 124.8, 124.9, 125.4, 126.2, 127.2, 128.7, 130.5, 134.5, 136.2, 137.0, 139.2, 146.6, 149.7, 154.1, 162.2; ESI-HRMS *m/z* calcd for $C_{33}H_{36}ClN_3O_3S$: 590.22387 $[M+H]^+$, 1179.44046 $[2M+H]^+$, found: 590.22411, 1179.43931.

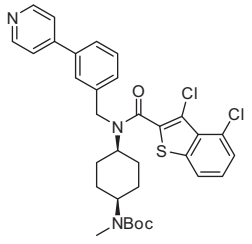

3.1.19. *tert*-Butyl (*cis*-4-{[(3,4-dichlorobenzo[*b*]thiophene-2-yl)-carbonyl](3-pyridin-4-yl benzyl)amino}cyclohexyl)methyl-carbamate 9b

Beige solid, 73% yield. Mp: 115–117 °C; IR (KBr): $\tilde{\nu}$ = 3434, 2932, 2862, 1686, 1638, 1594, 1446, 1148 cm^{-1}; ^1H NMR (300 MHz,

$(CD_3)_2SO$, 90 °C): δ = 1.35 (s, 9H), 1.47–1.63 (m, 4H), 1.78–1.84 (m, 4H), 2.60 (s, 3H), 3.59–3.72 (m, 1H), 3.80–3.88 (m, 1H), 4.80 (s, 2H), 7.44–7.57 (m, 4H), 7.59–7.61 (m, 2H), 7.63–7.67 (m, 1H), 7.70 (br, 1H), 8.03–8.06 (m, 1H), 8.63–8.65 (m, 2H); ^{13}C NMR (75 MHz, $(CD_3)_2SO$, 90 °C): δ = 27.7, 27.9, 28.5, 29.3, 46.1 (br), 53.2, 57.2, 78.0, 116.2, 120.6, 122.4, 124.8, 124.9, 126.6, 127.2, 127.4, 127.5, 128.7, 129.4, 133.2, 137.0, 138.9, 139.1, 146.6, 149.7, 154.2, 161.9; ESI-HRMS *m/z* calcd for $C_{33}H_{35}Cl_2N_3O_3S$: 624.18489 $[M+H]^+$, 1249.36251 $[2M+H]^+$, found: 624.18470, 1249.36258.

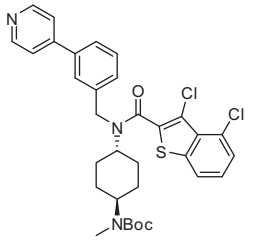

3.1.20. *tert*-Butyl (*trans*-4-{[(3,4-dichlorobenzo[*b*]thiophene-2-yl)carbonyl](3-pyridin-4-yl benzyl)amino}cyclohexyl)-methylcarbamate 9c

White solid, 63% yield. Mp: 104–105 °C; IR (KBr): $\tilde{\nu}$ = 3427, 2929, 1686, 1637, 1365, 1146 cm^{-1}; ^{1}H NMR (600 MHz, $(CD_3)_2SO$, 107 °C): δ = 1.35 (s, 9H), 1.53–1.55 (m, 2H), 1.65–1.67 (m, 2H), 1.83–1.87 (m, 4H), 2.63 (s, 3H), 3.63–3.65 (m, 1H), 3.90 (br, 1H), 4.80 (s, 2H), 7.44–7.50 (m, 3H), 7.54–7.57 (m, 3H), 7.62–7.63 (m, 1H), 7.68 (br, 1H), 7.99–7.99 (m, 1H), 8.63–8.66 (m, 2H); ^{13}C NMR (75 MHz, $CDCl_3$): δ = 28.6, 28.8, 29.7, 31.0, 45.3 (br), 52.9, 58.9, 79.7, 118.6, 121.9, 122.0, 125.7, 125.9, 126.4, 126.8, 127.9, 128.1, 129.5, 129.7, 132.3, 138.6, 138.9, 139.3, 148.4, 150.3, 155.6, 163.5; ESI-HRMS *m/z* calcd for $C_{33}H_{35}Cl_2N_3O_3S$: 624.18489 $[M+H]^+$, 1247.36251 $[2M+H]^+$, found: 624.18480, 1247.36346.

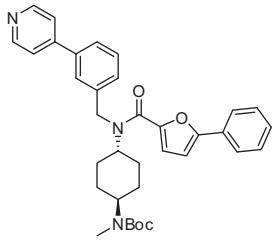

3.1.21. *tert*-Butyl methyl{*trans*-4-[(5-phenyl-2-furoyl)(3-pyridin-4-ylbenzyl)amino]-cyclohexyl}carbamate 9d

White solid, 98% yield. Mp: 114–115 °C; IR (KBr): $\tilde{\nu}$ = 2933, 1686, 1620, 1145 cm^{-1}; ^{1}H NMR (300 MHz, $(CD_3)_2SO$, 90 °C): δ = 1.37 (s, 9H), 1.52–1.66 (m, 4H), 1.72–1.87 (m, 4H), 2.65 (s, 3H), 3.66–3.76 (m, 1H), 4.23–4.31 (m, 1H), 4.87 (s, 2H), 6.96 (d, *J* = 3.6 Hz, 1H), 7.07 (d, *J* = 3.6 Hz, 1H), 7.26–7.33 (m, 3H), 7.43–7.51 (m, 4H), 7.58–7.60 (m, 2H), 7.63–7.65 (m, 1H), 7.71 (br, 1H), 8.58–8.60 (m, 2H); ^{13}C NMR (75 MHz, $(CD_3)_2SO$, 90 °C): δ = 27.7, 28.1, 28.2, 28.9, 46.5 (br), 53.2, 55.5, 77.9, 106.6, 117.4, 120.6, 123.5, 124.6, 126.9, 127.9, 128.3, 128.6, 129.0, 136.9, 140.4, 146.7, 147.0, 149.7, 153.8, 154.2, 159.7; ESI-HRMS *m/z* calcd for $C_{35}H_{39}N_3O_4$: 566.30133 $[M+H]^+$, 1131.59539 $[2M+H]^+$, 1153.57788 $[2M+Na]^+$, found: 566.30154, 1131.59551, 1153.57857.

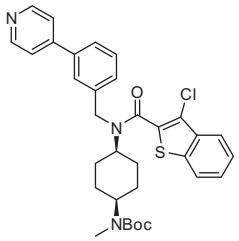

3.1.22. *tert*-Butyl (*cis*-4-{[(3-chlorobenzo[*b*]thiophene-2-yl)carbonyl](3-pyridin-4-yl benzyl)amino}cyclohexyl)-methylcarbamate 9e

Beige solid, 92% yield. Mp: 113–114 °C; IR (KBr): $\tilde{\nu}$ = 3432, 2931, 2862, 1686, 1636, 1593, 1440, 1364 cm^{-1}; ^{1}H NMR (300 MHz, $(CD_3)_2SO$, 90 °C): δ = 1.36 (s, 9H), 1.43–1.65 (m, 4H), 1.76–1.87 (m, 4H), 2.58 (s, 3H), 3.58–3.75 (m, 1H), 3.88 (br, 1H), 4.81 (s, 2H), 7.45–7.51 (m, 2H), 7.53–7.57 (m, 2H), 7.59–7.61 (m, 2H), 7.63–7.68 (m, 1H), 7.70 (br, 1H), 7.86–7.88 (m, 1H), 8.04–8.08 (m, 1H), 8.63–8.65 (m, 2H); ^{13}C NMR (75 MHz, $(CD_3)_2SO$, 90 °C): δ = 27.7, 27.9, 28.4, 29.4, 45.5 (br), 53.2, 57.4, 78.0, 117.2, 120.7, 121.5, 122.9, 124.8, 124.9, 125.4, 126.3, 127.2, 128.7, 130.6, 134.6, 136.2, 137.0, 139.2, 146.6, 149.7, 154.2, 162.2; ESI-HRMS *m/z* calcd for $C_{33}H_{36}ClN_3O_3S$: 590.22387 $[M+H]^+$, 1179.44046 $[2M+H]^+$, found: 590.22393, 1179.44096.

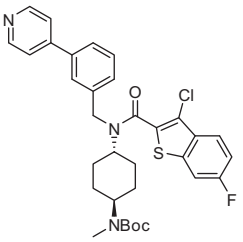

3.1.23. *tert*-Butyl (*trans*-4-{[(3-chloro-6-fluorobenzo[*b*]thiophene-2-yl)carbonyl](3-pyridin-4-ylbenzyl)amino}cyclohexyl)-methylcarbamate 9g

White solid, 96% yield. Mp: 98–99 °C; IR (KBr): $\tilde{\nu}$ = 3433, 2929, 2860, 1686, 1636, 1365, 1147 cm^{-1}; ^{1}H NMR (400 MHz, $CDCl_3$): δ = 1.41 (s, 9H), 1.54–2.04 (m, 8H), 2.59 (br, 3H), 3.66–4.01 (m, 2H), 4.82 (br, 2H), 7.21–7.60 (m, 7H), 7.70 (br, 1H), 7.84 (br, 1H), 8.66 (br, 2H); ^{19}F NMR (376 MHz, $CDCl_3$): δ = −113.8; ^{13}C NMR (100 MHz, $CDCl_3$): δ = 28.6, 28.9, 29.8, 31.1, 45.3 (br), 52.9, 59.0, 79.7, 109.2 (*J* = 26.3 Hz), 115.0 (*J* = 24.9 Hz), 117.4, 121.8, 124.2 (*J* = 9.1 Hz), 125.7, 125.9, 127.8, 129.5, 129.9, 132.4, 138.5 (*J* = 11.0 Hz), 138.6, 139.3, 148.4, 150.3, 155.6, 161.8 ($^1J_{CF}$ = 247 Hz), 163.5; ESI-HRMS *m/z* calcd for $C_{33}H_{35}ClFN_3O_3S$: 608.21445 $[M+H]^+$, found: 608.21404.

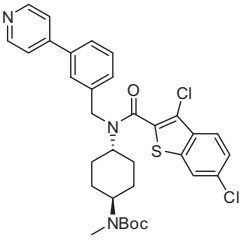

3.1.24. *tert*-Butyl (*trans*-4-{[(3,6-dichlorobenzo[*b*]thiophene-2-yl)carbonyl](3-pyridin-4-ylbenzyl)amino}cyclohexyl)-methylcarbamate 9h

Beige solid, 64% yield. Mp: 98–99 °C; IR (KBr): $\tilde{\nu}$ = 3434, 2930, 1686, 1637, 1592, 1365, 1147 cm^{-1}; ^1H NMR (400 MHz, $CDCl_3$): δ = 1.41 (s, 9H), 1.57–1.97 (m, 8H), 2.63 (br, 3H), 3.67–3.73 (m, 1H), 3.86 (br, 1H), 4.83 (br, 2H), 7.27–7.84 (m, 9H), 8.66 (br, 2H); ^{13}C NMR (75 MHz, $CDCl_3$): δ = 28.6, 28.9, 29.8, 31.1, 45.3 (br), 52.9, 59.1, 79.7, 119.1, 121.8, 122.5, 123.6, 125.7, 125.9, 126.7, 127.8, 129.6, 130.7, 133.1, 134.4, 138.4, 138.6, 139.3, 148.4, 150.3, 155.6, 163.4; ESI-HRMS *m/z* calcd for $C_{33}H_{35}Cl_2N_3O_3S$: 624.18489 $[M+H]^+$, 646.16684 $[M+Na]^+$, 1247.36251 $[2M+H]^+$, 1269.34446 $[2M+Na]^+$, found: 624.18507, 646.16650, 1247.36239, 1269.34288.

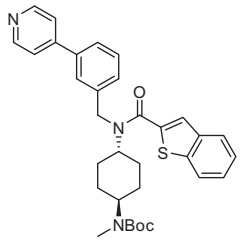

3.1.25. *tert*-Butyl (*trans*-4-{[(benzo[*b*]thiophene-2-yl)carbonyl](3-pyridin-4-ylbenzyl)amino} cyclohexyl)methylcarbamate 9i

Yellow oil, 50% yield. ^1H NMR (300 MHz, $(CD_3)_2SO$, 90 °C): δ = 1.40 (s, 9H), 1.50–1.62 (m, 4H), 1.81–1.91 (m, 4H), 2.62 (s, 3H), 3.75–3.89 (m, 1H), 4.24–4.34 (m, 1H), 4.87 (s, 2H), 7.18 (d, *J* = 7.8 Hz, 1H), 7.39–7.51 (m, 5H), 7.60–7.66 (m, 5H), 8.62–8.64 (m, 2H); ^{13}C NMR (75 MHz, $(CD_3)_2SO$, 90 °C): δ = 27.7, 28.0, 28.3, 30.4, 45.5 (br), 53.1, 56.7, 78.1, 120.8, 124.8, 125.2, 125.3, 125.4, 127.2, 127.7, 128.7, 128.8, 136.2, 136.9, 137.1, 138.3, 139.8, 146.6, 149.6, 154.2, 164.2; ESI-HRMS *m/z* calcd for $C_{33}H_{37}N_3O_3S$: 556.26284 $[M+H]^+$, found: 556.26290.

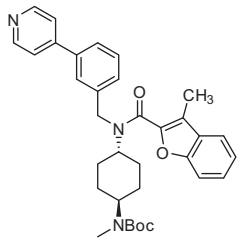

3.1.26. *tert*-Butyl methyl(*trans*-4-{[(3-methylbenzo[*b*]furan-2-yl)carbonyl](3-pyridin-4-ylbenzyl)amino}cyclohexyl)-carbamate 9j

Colorless oil, 86% yield. ^1H NMR (600 MHz, $(CD_3)_2SO$, 107 °C): δ = 1.39 (s, 9H), 1.57–1.59 (m, 2H), 1.67–1.69 (m, 2H), 1.82–1.88 (m, 4H), 2.24 (s, 3H), 2.65 (s, 3H), 3.63–3.72 (m, 1H), 4.00–4.10 (m, 1H), 4.80 (s, 2H), 7.28–7.31 (m, 1H), 7.37–7.40 (m, 1H), 7.41–7.47 (m, 3H), 7.52–7.53 (m, 2H), 7.58–7.59 (m, 1H), 7.62–7.64 (m, 2H), 8.60–8.61 (m, 2H); ^{13}C NMR (75 MHz, $(CD_3)_2SO$, 90 °C): δ = 7.8, 27.6, 27.9, 28.4, 29.3, 46.3 (br), 53.1, 56.9, 78.0, 110.8, 117.9, 119.9, 120.7, 122.9, 124.8, 124.9, 125.7, 127.2, 128.1, 128.7, 136.8, 139.7, 144.3, 146.7, 149.8, 152.5, 154.5, 161.7; ESI-HRMS *m/z* calcd for $C_{34}H_{39}N_3O_4$: 554.30133 $[M+H]^+$, found: 554.30186.

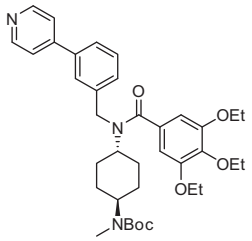

3.1.27. *tert*-Butyl methyl{*trans*-4-[(3-pyridin-4-ylbenzyl)(3,4,5-triethoxybenzoyl)-amino] cyclohexyl}carbamate 9k

Yellow solid, 84% yield. Mp: 73–75 °C; IR (KBr): $\tilde{\nu}$ = 2976, 2932, 2360, 2340, 1684, 1652, 1123 cm^{-1}; ^1H NMR (300 MHz, $(CD_3)_2SO$, 90 °C): δ = 1.22 (t, *J* = 6.7 Hz, 3H), 1.27 (t, *J* = 6.6 Hz, 6H), 1.35 (s, 9H), 1.41–1.50 (m, 2H), 1.56–1.61 (m, 2H), 1.68–1.80 (m, 4H), 2.60 (s, 3H), 3.57–3.69 (m, 1H), 3.82–3.89 (m, 1H), 3.96 (q, *J* = 7.0 Hz, 2H), 3.97 (q, *J* = 6.9 Hz, 4H), 4.65 (s, 2H), 6.61 (s, 2H), 7.37–7.49 (m, 2H), 7.61–7.63 (m, 4H), 8.61–8.63 (m, 2H); ^{13}C NMR (75 MHz, $(CD_3)_2SO$, 90 °C): δ = 14.1, 14.8, 27.7, 28.1, 28.3, 29.0, 46.0 (br), 53.3, 56.2, 64.1, 67.6, 78.0, 105.4, 120.7, 124.6, 124.7, 127.2, 128.7, 131.8, 136.8, 138.4, 140.3, 146.7, 149.7, 151.9, 154.2, 170.5; ESI-HRMS *m/z* calcd for $C_{37}H_{49}N_3O_6$: 632.36941 $[M+H]^+$, 1263.73155 $[2M+H]^+$, found: 632.36974, 1263.73238.

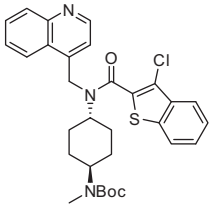

3.1.28. *tert*-Butyl (*trans*-4-{[(3-chlorobenzo[*b*]thiophene-2-yl)carbonyl](quinolin-4-yl methyl)amino}cyclohexyl)-methylcarbamate 9l

Yellow oil, 76% yield. ^1H NMR (300 MHz, $(CD_3)_2SO$, 90 °C): δ = 1.31 (s, 9H), 1.45–1.58 (m, 4H), 1.69–1.95 (m, 4H), 2.55 (s, 3H), 3.55–3.69 (m, 1H), 3.88–4.04 (m, 1H), 5.23 (s, 2H), 7.49 (d, *J* = 4.5 Hz, 1H), 7.53–7.57 (m, 2H), 7.60–7.65 (m, 1H), 7.73–7.78 (m, 1H), 7.85–7.88 (m, 1H), 8.03–8.06 (m, 2H), 8.19–8.22 (m, 1H), 8.89 (d, *J* = 4.5 Hz, 1H); ^{13}C NMR (75 MHz, $(CD_3)_2SO$, 90 °C): δ = 27.7, 27.8, 28.4, 29.1, 43.0 (br), 53.0, 57.3, 77.9, 117.6, 121.5, 122.8, 122.9, 125.2, 125.4, 126.0, 126.3, 128.7, 129.2, 130.1, 134.5, 136.2, 143.1, 147.3, 149.5, 154.1, 162.4; ESI-HRMS *m/z* calcd for $C_{31}H_{34}ClN_3O_3S$: 564.20822 $[M+H]^+$, 1127.40916 $[2M+H]^+$, found: 564.20767, 1127.40857.

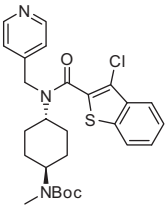

3.1.29. *tert*-Butyl (*trans*-4-{[(3-chlorobenzo[*b*]thiophene-2-yl)carbonyl](pyridin-4-ylmethyl) amino}cyclohexyl)-methylcarbamate 9m

Colorless oil, 76% yield. ^1H NMR (300 MHz, $(CD_3)_2SO$, 90 °C): δ = 1.34 (s, 9H), 1.45–1.63 (m, 4H), 1.71–1.82 (m, 4H), 2.56 (s,

3H), 3.57–3.72 (m, 1H), 3.76–3.92 (m, 1H), 4.73 (s, 2H), 7.33–7.35 (m, 2H), 7.53–7.61 (m, 2H), 7.85–7.88 (m, 1H), 8.06–8.08 (m, 1H), 8.51–8.53 (m, 2H); ^{13}C NMR (75 MHz, $(CD_3)_2SO$, 90 °C): δ = 27.7, 27.8, 28.4, 29.3, 45.0 (br), 53.0, 57.2, 78.0, 117.4, 121.5, 121.6, 122.9, 125.5, 126.3, 130.1, 134.5, 136.2, 147.4, 148.9, 154.1, 162.2; ESI-HRMS *m/z* calcd for $C_{27}H_{32}ClN_3O_3S$: 514.19257 $[M+H]^+$, 1027.37786 $[2M+H]^+$, found: 514.19215, 1027.37744.

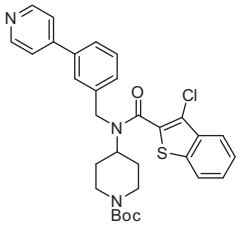

3.1.30. *tert*-Butyl 4-{[(3-chlorobenzo[*b*]thiophene-2-yl)carbonyl](3-pyridin-4-ylbenzyl) amino}piperidine-1-carboxylate 13a

White solid, 78% yield. Mp: 63–65 °C; ^{1}H NMR (400 MHz, $CDCl_3$): δ = 1.41 (s, 9H), 1.68–1.74 (m, 4H), 2.52–2.83 (m, 2H), 3.93–4.13 (m, 3H), 4.83 (br, 2H), 7.27–7.87 (m, 10H), 8.66 (br, 2H); ^{13}C NMR (100 MHz, $CDCl_3$): δ = 28.5, 31.2, 43.2, 45.7 (br), 58.4, 80.0, 119.3, 121.8, 122.7, 122.9, 125.6, 125.8, 126.8, 127.6, 129.6, 130.2, 135.7, 137.4, 138.7, 139.0, 148.6, 150.3, 154.6, 164.2; ESI-HRMS *m/z* calcd for $C_{31}H_{32}ClN_3O_3S$: 562.19257 $[M+H]^+$, 584.17451 $[M+Na]^+$, found: 562.19286, 584.17484.

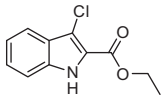

3.1.31. Ethyl 3-chloro-1*H*-indole-2-carboxylate 20

To a solution of ethyl 1*H*-indole-2-carboxylate (1.00 g, 5.29 mmol, 1.0 equiv) in benzene (50 ml) was added slowly sulfuryl chloride (1.78 g, 1.07 ml, 13.2 mmol, 2.5 equiv) and the solution was heated to reflux for 3.5 h. After removal of the solvent under reduced pressure, the crude product was purified by column chromatography (*n*-hexane/EtOAc 4:1, v/v) to give **20** as a white solid (1.01 g, 85%); mp: 158 °C; IR (KBr): $\tilde{\nu}$ = 3294, 2982, 1683, 1522, 1335, 1257, 744 cm^{-1}; ^{1}H NMR (400 MHz, $CDCl_3$): δ = 1.47 (t, *J* = 7.2 Hz, 3H), 4.49 (q, *J* = 7.2 Hz, 2H), 7.22 (ddd, *J* = 8.0, 6.2, 1.7 Hz, 1H), 7.35–7.41 (m, 2H), 7.72 (dd, *J* = 8.2, 1.0 Hz, 1H), 9.24 (br, 1H); ^{13}C NMR (100 MHz, $CDCl_3$): δ = 14.5, 61.6, 112.2, 112.5, 120.3, 121.4, 122.5, 126.3, 126.7, 135.0, 161.3; ESI-HRMS *m/z* calcd for $C_{11}H_{10}ClNO_2$: 246.02923 $[M+Na]^+$, 469.06923 $[2M+Na]^+$, found: 246.02913, 469.06860.

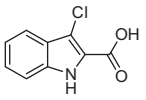

3.1.32. 3-Chloro-1*H*-indole-2-carboxylic acid 21

To a solution of ethyl 3-chloro-1*H*-indole-2-carboxylate **20** (1.5 g, 6.71 mmol, 1.0 equiv) in EtOH (30 ml) was added a 5 N solution of NaOH (6 ml) and the resulting solution was heated to reflux for 50 min. After cooling down to rt diluted H_2SO_4 was added until an acidic pH-value was achieved. The mixture was extracted with CH_2Cl_2 (3 × 50 ml) and the combined organic layers were dried over Na_2SO_4. The solvent was removed under reduced pressure and **21** was obtained as a brown solid (1.31 g, quantitative); mp: 192–194 °C; IR (KBr): $\tilde{\nu}$ = 3418, 1670, 1536, 1243, 742 cm^{-1}; ^{1}H NMR (300 MHz, $(CD_3)_2SO$): δ = 7.15 (ddd, *J* = 8.0, 6.9, 1.0 Hz, 1H), 7.32 (ddd, *J* = 8.3, 6.9, 1.2 Hz, 1H), 7.45 (d, *J* = 8.3 Hz, 1H), 7.57 (d, *J* = 8.1 Hz, 1H), 11.99 (s, 1H), 13.35 (br, 1H); ^{13}C NMR (75 MHz, $(CD_3)_2SO$): δ = 109.1, 113.0, 118.9, 120.8, 123.2, 125.1, 125.6, 134.9, 161.5; ESI-HRMS *m/z* calcd for $C_9H_6ClNO_2$: 217.99793 $[M+Na]^+$, 413.00663 $[2M+Na]^+$, found: 217.99808, 413.00694.

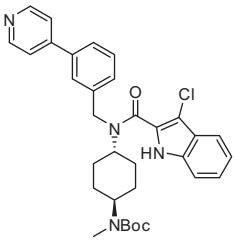

3.1.33. *tert*-Butyl (*trans*-4-{[(3-chloro-1*H*-indol-2-yl)carbonyl](3-pyridin-4-ylbenzyl) amino}cyclohexyl)methylcarbamate 9f

A mixture of 3-chloro-1*H*-indole-2-carboxylic acid **21** (22.8 mg, 116 μmol, 1.0 equiv) and PyBOP reagent (46.1 mg, 116 μmol, 1.0 equiv) in dry DMF (100 μl) was treated with NEt_3 (48.6 μl, 350 μmol, 3.0 equiv) and the mixture was stirred at rt for 15 min. After adding a solution of *tert*-butyl methyl{*trans*-4-[(3-pyridin-4-ylbenzyl)amino]cyclohexyl}carbamate **8a** (46.1 mg, 116 μmol, 1.0 equiv) in dry DMF (200 μl) the mixture was stirred at rt for 36 h and additional 12 h at 50 °C. The reaction mixture was diluted with water (2 ml), extracted with CH_2Cl_2 (3 × 2 ml) and the combined organic layers were dried over Na_2SO_4. After removal of the solvent under reduced pressure, the crude product was purified by column chromatography (CH_2Cl_2/MeOH 50:1 → 10:1, v/v) to give **9f** as a yellow solid (33.5 mg, 50%); mp: 83–85 °C; ^{1}H NMR (400 MHz, $CDCl_3$): δ = 1.42 (s, 9H), 1.62–1.75 (m, 4H), 1.86–1.90 (m, 4H), 2.63 (s, 3H), 3.91 (br, 1H), 4.20 (br, 1H), 4.81 (s, 2H), 7.18–7.25 (m, 3H), 7.42–7.50 (m, 5H), 7.58–7.67 (m, 2H), 8.65 (br, 2H), 9.83 (br, 1H); ^{13}C NMR (100 MHz, $CDCl_3$): δ = 28.6, 28.9, 29.8, 31.9, 46.4 (br), 57.1, 58.9, 79.7, 105.6, 112.3, 117.3, 119.1, 121.2, 122.3, 125.0, 125.2, 125.4, 127.0, 128.3, 129.7, 135.3, 137.7, 139.7, 148.5, 150.3, 155.7, 164.3; ESI-HRMS *m/z* calcd for $C_{33}H_{37}ClN_4O_3$: 573.26270 $[M+H]^+$, 595.24464 $[M+Na]^+$, found: 573.26302, 595.24551.

3.1.34. General procedure for preparing amides 10a, 10b, 10c, 10d, 10e, 10f, 10g, 18, 10h, 10i, 10j, 10k, 10l, 10m and 14a

Carbamate (1.0 equiv) or carboxylate (1.0 equiv) was dissolved in dry CH_2Cl_2 and trifluoroacetic acid (30 equiv) was added dropwise. The solution was stirred at rt until the end of the reaction was monitored by TLC. After removal of the solvent the residue was dissolved in CH_2Cl_2, washed four to five times with 1 N NaOH solution and dried over Na_2SO_4. The solvent was removed under reduced pressure to obtain the corresponding amide as pure product.

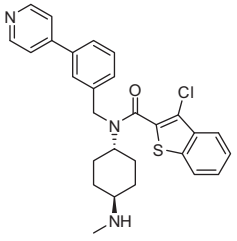

3.1.35. 3-Chloro-*N*-[*trans*-4-(methylamino)cyclohexyl]-*N*-(3-pyridin-4-ylbenzyl)benzo[*b*]- thiophene-2-carboxamide 10a[16]

White solid, quantitative yield. Mp: 109–111 °C; IR (KBr): $\tilde{\nu}$ = 2932, 1634, 1593, 1409, 756 cm^{-1}; ^1H NMR (300 MHz, $(CD_3)_2SO$, 90 °C): δ = 0.82–0.89 (m, 2H), 1.62–1.74 (m, 4H), 1.83–1.87 (m, 2H), 2.12 (br, 1H), 2.18 (s, 3H), 3.85 (br, 1H), 4.78 (s, 2H), 7.43–7.48 (m, 2H), 7.50–7.53 (m, 1H), 7.53–7.55 (m, 1H), 7.57–7.59 (m, 2H), 7.60–7.64 (m, 1H), 7.69 (br, 1H), 7.82–7.85 (m, 1H), 8.01–8.04 (m, 1H), 8.61–8.63 (m, 2H); ^{13}C NMR (75 MHz, $(CD_3)_2SO$, 90 °C): δ = 29.0, 31.2, 32.7, 45.6 (br), 56.4, 58.1, 117.2, 120.6, 121.5, 122.8, 124.8, 124.9, 125.4, 126.2, 127.2, 128.7, 130.6, 134.5, 136.2, 137.0, 139.2, 146.6, 149.7, 162.2; ESI-HRMS *m/z* calcd for $C_{28}H_{28}ClN_3OS$: 490.17144 $[M+H]^+$, found: 490.17142.

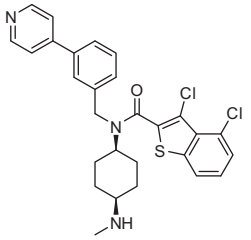

3.1.36. 3,4-Dichloro-*N*-[*cis*-4-(methylamino)cyclohexyl]-*N*-(3-pyridin-4-ylbenzyl)-benzo[*b*]thiophene-2-carboxamide 10b

Light yellow solid, quantitative yield. Mp: 97–99 °C; IR (KBr): $\tilde{\nu}$ = 3427, 2928, 2853, 1634, 1593, 1445, 1403, 779 cm^{-1}; ^1H NMR (300 MHz, $(CD_3)_2SO$, 90 °C): δ = 0.78–0.98 (m, 2H), 1.68–1.75 (m, 4H), 1.86–1.90 (m, 2H), 2.19–2.27 (m, 4H), 3.82 (br, 1H), 4.76 (s, 2H), 7.43–7.53 (m, 4H), 7.56–7.59 (m, 2H), 7.61–7.65 (m, 1H), 7.67 (br, 1H), 8.01–8.04 (m, 1H), 8.61–8.63 (m, 2H); ^{13}C NMR (75 MHz, $(CD_3)_2SO$, 90 °C): δ = 28.9, 30.9, 32.4, 45.8 (br), 56.4, 58.3, 116.2, 120.7, 122.4, 124.8, 124.9, 126.7, 127.2, 127.4, 127.6, 128.7, 129.4, 133.2, 137.0, 138.8, 139.1, 146.6, 149.8, 161.9; ESI-HRMS *m/z* calcd for $C_{28}H_{27}Cl_2N_3OS$: 524.13247 $[M+H]^+$, found: 524.13235.

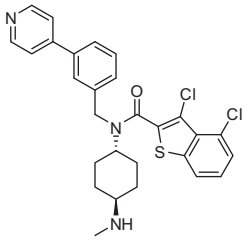

3.1.37. 3,4-Dichloro-*N*-[*trans*-4-(methylamino)cyclohexyl]-*N*-(3-pyridin-4-ylbenzyl)-benzo[*b*]thiophene-2-carboxamide 10c

Beige solid, quantitative yield. Mp: 86–88 °C; IR (KBr): $\tilde{\nu}$ = 3425, 2931, 2854, 1635, 1594, 1446, 1404, 780 cm^{-1}; ^1H NMR (300 MHz, $(CD_3)_2SO$, 90 °C): δ = 0.86–0.96 (m, 2H), 1.67–1.75 (m, 4H), 1.82–1.92 (m, 2H), 2.18 (br, 1H), 2.20 (s, 3H), 3.80 (br, 1H), 4.76 (s, 2H), 7.43–7.54 (m, 4H), 7.56–7.59 (m, 2H), 7.61–7.65 (m, 1H), 7.68 (br, 1H), 8.01–8.04 (m, 1H), 8.61–8.63 (m, 2H); ^{13}C NMR (75 MHz, $(CD_3)_2SO$, 90 °C): δ = 28.8, 30.5, 32.2, 45.6 (br), 56.3, 57.7, 116.2, 120.6, 122.4, 124.8, 124.9, 126.7, 127.2, 127.4, 127.6, 128.7, 129.3, 133.2, 137.0, 138.8, 139.1, 146.6, 149.8, 161.9; ESI-HRMS *m/z* calcd for $C_{28}H_{27}Cl_2N_3OS$: 524.13247 $[M+H]^+$, 1047.25765 $[2M+H]^+$, found: 524.13261, 1047.25846.

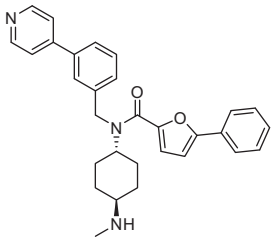

3.1.38. *N*-[*trans*-4-(Methylamino)cyclohexyl]-5-phenyl-*N*-(3-pyridin-4-ylbenzyl)-2-furamide 10d

White solid, quantitative. Mp: 81–83 °C; IR (KBr): $\tilde{\nu}$ = 3432, 2930, 2853, 1619, 1480, 1449, 1409, 762 cm^{-1}; ^1H NMR (300 MHz, $(CD_3)_2SO$, 90 °C): δ = 1.00–1.15 (m, 2H), 1.61–1.82 (m, 4H), 1.87–1.99 (m, 2H), 2.18–2.24 (m, 1H), 2.26 (s, 3H), 4.20–4.33 (m, 1H), 4.84 (s, 2H), 6.96 (d, *J* = 3.6 Hz, 1H), 7.06 (d, *J* = 3.6 Hz, 1H), 7.26–7.36 (m, 3H), 7.39–7.51 (m, 4H), 7.57–7.59 (m, 2H), 7.61–7.64 (m, 1H), 7.69 (br, 1H), 8.58–8.60 (m, 2H); ^{13}C NMR (75 MHz, $(CD_3)_2SO$, 90 °C): δ = 28.6, 31.2, 32.6, 46.3 (br), 56.3, 56.7, 106.6, 117.3, 120.7, 123.5, 124.6, 126.9, 127.9, 128.3, 128.6, 129.0, 136.9, 140.4, 146.7, 147.1, 149.7, 153.8, 159.8; ESI-HRMS *m/z* calcd for $C_{30}H_{31}N_3O_2$: 466.24890 $[M+H]^+$, 931.49053 $[2M+H]^+$, found: 466.24937, 931.49062.

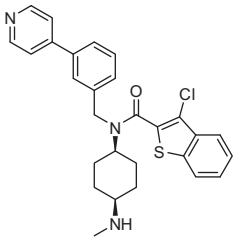

3.1.39. 3-Chloro-*N*-[*cis*-4-(methylamino)cyclohexyl]-*N*-(3-pyridin-4-ylbenzyl)benzo[*b*]-thiophene-2-carboxamide 10e

Beige solid, quantitative yield. Mp: 93–94 °C; IR (KBr): $\tilde{\nu}$ = 3426, 2928, 2853, 1633, 1593, 1411, 782, 756 cm^{-1}; ^1H NMR (300 MHz, $(CD_3)_2SO$, 90 °C): δ = 0.81–0.96 (m, 2H), 1.66–1.79 (m, 4H), 1.80–2.02 (m, 2H), 2.07–2.16 (m, 1H), 2.20 (s, 3H), 3.85 (br, 1H), 4.79 (s, 2H), 7.44–7.49 (m, 2H), 7.51–7.57 (m, 2H), 7.59–7.61 (m, 2H), 7.63–7.67 (m, 1H), 7.70 (br, 1H), 7.85–7.87 (m, 1H), 8.03–8.05 (m, 1H), 8.63–8.65 (m, 2H); ^{13}C NMR (75 MHz, $(CD_3)_2SO$, 90 °C): δ = 29.0, 31.0, 32.5, 45.5 (br), 56.4, 58.1, 117.2, 120.7, 121.5, 122.9, 124.8, 124.9, 125.5, 126.3, 127.3, 128.7, 130.6, 134.5, 136.2, 137.0, 139.2, 146.6, 149.8, 162.5; ESI-HRMS *m/z* calcd for $C_{28}H_{28}ClN_3OS$: 490.17144 $[M+H]^+$, 979.33566 $[2M+H]^+$, found: 490.17187, 979.33599.

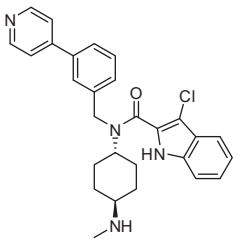

3.1.40. 3-Chloro-*N*-[*trans*-4-(methylamino)cyclohexyl]-*N*-(3-pyridin-4-ylbenzyl)-1*H*-indole-2-carboxamide 10f

Yellow solid, quantitative yield. Mp: 149–151 °C; IR (KBr): $\tilde{\nu}$ = 2923, 1691, 1628, 1601, 1384, 1201, 1175, 1131, 747 cm^{-1}; ^1H NMR (300 MHz, $(CD_3)_2SO$, 90 °C): δ = 1.17–1.25 (m, 2H), 1.73–1.81 (m, 4H), 1.99–2.02 (m, 2H), 2.43 (s, 3H), 2.72–2.84 (m, 1H), 3.80–3.96 (m, 1H), 4.78 (s, 2H), 7.13–7.18 (m, 1H), 7.23–7.28 (m, 1H), 7.41–7.55 (m, 4H), 7.58–7.60 (m, 2H), 7.61–7.64 (m, 1H), 7.67 (br, 1H), 8.61–8.63 (m, 2H), 11.77 (br, 1H); ^{13}C NMR (75 MHz, $(CD_3)_2SO$, 90 °C): δ = 27.6, 28.1, 29.8, 46.0 (br), 55.4, 57.5, 101.6, 112.0, 117.3, 120.1, 120.7, 123.2, 123.8, 124.8, 124.9, 127.2, 128.6, 130.0, 134.2, 137.0, 139.3, 146.6, 149.7, 162.7; ESI-HRMS *m/z* calcd for $C_{28}H_{29}ClN_4OS$: 473.21027 $[M+H]^+$, found: 473.21011.

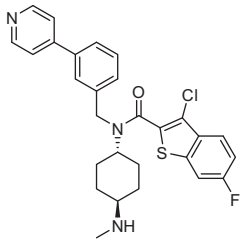

3.1.41. 3-Chloro-6-fluoro-*N*-[*trans*-4-(methylamino)cyclohexyl]-*N*-(3-pyridin-4-ylbenzyl) benzo[*b*]thiophene-2-carboxamide 10g

Beige solid, quantitative yield. Mp: 85–86 °C; IR (KBr): $\tilde{\nu}$ = 3425, 2930, 2855, 1633, 1604, 1594, 1468, 1416 cm^{-1}; ^1H NMR (300 MHz, $(CD_3)_2SO$, 90 °C): δ = 0.81–1.00 (m, 2H), 1.68–1.75 (m, 4H), 1.83–1.92 (m, 2H), 2.15 (br, 1H), 2.21 (s, 3H), 3.86 (br, 1H), 4.77 (s, 2H), 7.38–7.51 (m, 3H), 7.57–7.59 (m, 2H), 7.61–7.69 (m, 2H), 7.86 (dd, *J* = 8.9, 5.0 Hz, 1H), 7.94–7.98 (m, *J* = 9.0, 2.3 Hz, 1H), 8.62–8.64 (m, 2H); ^{19}F NMR (282 MHz, $(CD_3)_2SO$): δ = −114.2; ^{13}C NMR (75 MHz, $(CD_3)_2SO$, 90 °C): δ = 29.0, 31.1, 32.6, 45.6 (br), 56.4, 58.2, 109.3 (*J* = 26.4 Hz), 114.5 (*J* = 24.7 Hz), 117.1, 120.7, 123.3 (*J* = 9.9 Hz), 124.8, 124.9, 127.2, 128.7, 129.8, 131.3, 137.0, 137.4 (*J* = 11.0 Hz), 139.2, 146.6, 149.8, 160.7 (*J* = 244 Hz), 162.4; ESI-HRMS *m/z* calcd for $C_{28}H_{27}ClFN_3OS$: 508.16202 $[M+H]^+$, found: 508.16205.

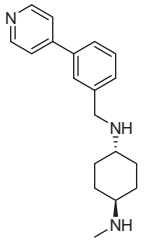

3.1.42. *trans*-*N*-Methyl-*N*′-(3-pyridin-4-ylbenzyl)cyclohexane-1,4-diamine 18

Yellow oil, quantitative yield. IR (film in CCl_4): $\tilde{\nu}$ = 3438, 2927, 1594, 1383, 785, 761 cm^{-1}; ^1H NMR (300 MHz, $(CD_3)_2SO$, 90 °C): δ = 1.12–1.24 (m, 3H), 1.74–1.87 (m, 2H), 1.94–2.04 (m, 5H), 2.29 (s, 3H), 2.33–2.41 (m, 1H), 4.35 (tt, *J* = 11.9, 3.6 Hz, 1H), 4.86 (s, 2H), 7.17 (dd, *J* = 7.7, 0.6 Hz, 1H), 7.43 (t, *J* = 7.7 Hz, 1H), 7.49 (s, 1H), 7.58–7.60 (m, 2H), 7.61–7.64 (m, 1H), 8.61–8.63 (m, 2H); ^{13}C NMR (75 MHz, $(CD_3)_2SO$, 90 °C): δ = 29.9, 30.6, 32.6, 45.6, 56.6, 61.9, 120.7, 125.1, 125.3, 127.6, 128.8, 136.2, 137.1, 146.4, 149.8; ESI-HRMS *m/z* calcd for $C_{19}H_{25}N_3$: 296.21204 $[M+H]^+$, found: 296.21210.

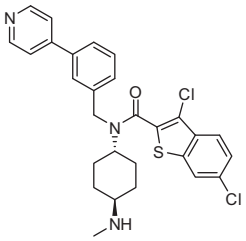

3.1.43. 3,6-Dichloro-*N*-[*trans*-4-(methylamino)cyclohexyl]-*N*-(3-pyridin-4-ylbenzyl)benzo[*b*]thiophene-2-carboxamide 10h

Beige solid, quantitative yield. Mp: 86–88 °C; IR (KBr): $\tilde{\nu}$ = 3433, 2928, 2854, 1633, 1591, 1478, 1415, 780 cm^{-1}; ^1H NMR (300 MHz, $(CD_3)_2SO$, 90 °C): δ = 0.97–1.16 (m, 2H), 1.68–1.83 (m, 4H), 1.85–1.98 (m, 2H), 2.27 (s, 3H), 2.35–2.47 (m, 1H), 3.86 (br, 1H), 4.77 (s, 2H), 7.42–7.52 (m, 2H), 7.58–7.61 (m, 3H), 7.63–7.68 (m, 2H), 7.83–7.86 (m, 1H), 8.21–8.22 (m, 1H), 8.63–8.65 (m, 2H); ^{13}C NMR (100 MHz, $(CD_3)_2SO$): δ = 29.3, 29.8, 30.0, 44.4 (br), 56.1, 58.9, 117.3, 121.2, 123.3, 123.4, 125.0, 125.2, 126.7, 127.5, 129.3, 131.7, 132.3, 133.7, 137.3, 137.8, 139.6, 147.0, 150.3, 162.1; ESI-HRMS *m/z* calcd for $C_{28}H_{27}Cl_2N_3OS$: 524.13247 $[M+H]^+$, 1047.25765 $[2M+H]^+$, found: 524.13261, 1047.25722.

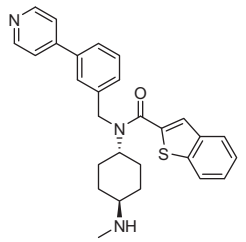

3.1.44. *N*-[*trans*-4-(Methylamino)cyclohexyl]-*N*-(3-pyridin-4-ylbenzyl)-benzo[*b*]thiophene-2-carboxamide 10i

Yellow oil, quantitative yield. IR (film in CCl_4): $\tilde{\nu}$ = 2937, 2857, 1595, 446, 381, 786 cm^{-1}; ^1H NMR (300 MHz, $(CD_3)_2SO$, 90 °C): δ = 1.15–1.25 (m, 2H), 1.72–1.86 (m, 2H), 1.97–2.01 (m, 4H), 2.29 (s, 3H), 2.33–2.40 (m, 1H), 4.25 (tt, *J* = 12.0, 3.6 Hz, 1H), 4.86 (s, 2H), 7.17 (d, *J* = 7.7 Hz, 1H), 7.38–7.50 (m, 5H), 7.58–7.73 (m, 5H), 8.61–8.64 (m, 2H); ^{13}C NMR (75 MHz, $(CD_3)_2SO$, 90 °C): δ = 29.9, 30.7, 32.6, 45.6 (br), 56.7, 61.9, 120.7, 125.1, 125.4, 125.6, 125.8, 127.6, 128.0, 128.8, 129.0, 136.2, 137.1, 137.3, 138.0, 139.8, 146.4, 149.8, 164.2; ESI-HRMS *m/z* calcd for $C_{28}H_{29}N_3OS$: 456.21041 $[M+H]^+$, found: 456.21040.

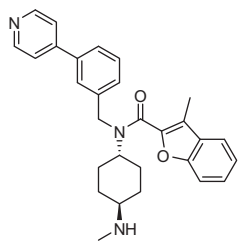

3.1.45. 3-Methyl-*N*-[*trans*-4-(methylamino)cyclohexyl]-*N*-(3-pyridin-4-ylbenzyl)benzo[*b*]-furan-2-carboxamide 10j

Yellow solid, quantitative yield. Mp: 45 °C; IR (KBr): $\tilde{\nu}$ = 3417, 2926, 2855, 1627, 1593, 1446, 1418, 1260, 746 cm^{-1}; ^1H NMR (300 MHz, $(CD_3)_2SO$, 90 °C): δ = 0.93–1.10 (m, 2H), 1.64–1.82 (m,

4H), 1.90–1.99 (m, 2H), 2.17–2.25 (m, 1H), 2.27 (s, 3H), 2.34 (s, 3H), 4.03 (br, 1H), 4.80 (s, 2H), 7.30–7.34 (m, 1H), 7.38–7.55 (m, 4H), 7.57–7.59 (m, 2H), 7.61–7.69 (m, 3H), 8.63–8.65 (m, 2H); ^{13}C NMR (75 MHz, $(CD_3)_2SO$, 90 °C): δ = 7.7, 29.0, 31.3, 32.7, 46.2 (br), 56.7, 61.9, 110.8, 117.8, 120.0, 120.6, 122.7, 124.7, 124.8, 125.7, 127.1, 128.1, 128.6, 136.9, 139.8, 144.4, 146.7, 149.7, 152.4, 161.7; ESI-HRMS *m/z* calcd for $C_{29}H_{31}N_3O_2$: 454.24890 $[M+H]^+$, 907.49053 $[2M+H]^+$, found: 454.24899, 907.49191.

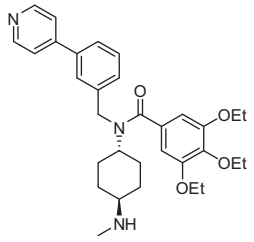

3.1.46. 3,4,5-Triethoxy-*N*-[*trans*-4-(methylamino)cyclohexyl]-*N*-(3-pyridin-4-ylbenzyl) benzamide 10k

White solid, 73% yield. Mp: 80–81 °C; IR (KBr): $\tilde{\nu}$ = 3427, 2976, 2930, 2856, 1631, 1593, 1579, 1478 cm^{-1}; ^{1}H NMR (300 MHz, $(CD_3)_2SO$, 90 °C): δ = 0.84–0.97 (m, 2H), 1.22 (t, *J* = 7.0 Hz, 3H), 1.27 (t, *J* = 6.9 Hz, 6H), 1.57–1.76 (m, 4H), 1.84–1.91 (m, 2H), 2.12–2.20 (m, 1H), 2.22 (s, 3H), 3.84 (br, 1H), 3.96 (q, *J* = 7.0 Hz, 2H), 3.97 (q, *J* = 6.9 Hz, 4H), 4.63 (s, 2H), 6.60 (s, 2H), 7.37–7.49 (m, 2H), 7.60–7.62 (m, 4H), 8.61–8.63 (m, 2H); ^{13}C NMR (300 MHz, $(CD_3)_2SO$, 90 °C): δ = 14.1, 14.8, 28.7, 31.2, 32.6, 45.6 (br), 56.6, 57.1, 64.1, 67.6, 105.4, 120.6, 124.5, 124.7, 127.1, 128.6, 131.8, 136.8, 138.4, 140.3, 146.7, 149.7, 151.9, 170.5; ESI-HRMS *m/z* calcd for $C_{32}H_{41}N_3O_4$: 532.31698 $[M+H]^+$, 1063.62669 $[2M+H]^+$, found: 532.31662, 1063.62604.

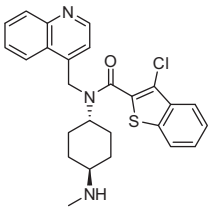

3.1.47. 3-Chloro-*N*-[*trans*-4-(methylamino)cyclohexyl]-*N*-(quinolin-4-ylmethyl)benzo[*b*]- thiophene-2-carboxamide 10l

White solid, quantitative yield. Mp: 88–90 °C; IR (KBr): $\tilde{\nu}$ = 3431, 2930, 2854, 1635, 1409, 1294, 756 cm^{-1}; ^{1}H NMR (300 MHz, $(CD_3)_2SO$, 90 °C): δ = 0.84–0.95 (m, 2H), 1.62–1.73 (m, 2H), 1.82–1.86 (m, 4H), 2.12 (br, 1H), 2.17 (s, 3H), 3.92 (br, 1H), 5.20 (s, 2H), 7.49 (d, *J* = 4.5 Hz, 1H), 7.53–7.58 (m, 2H), 7.60–7.65 (m, 1H), 7.73–7.78 (m, 1H), 7.85–7.88 (m, 1H), 8.03–8.06 (m, 2H), 8.19–8.21 (m, 1H), 8.89 (d, *J* = 4.2 Hz, 1H); ^{13}C NMR (75 MHz, $(CD_3)_2SO$, 90 °C): δ = 28.7, 31.0, 32.6, 42.4 (br), 56.2, 58.3, 117.6, 121.5, 122.8, 122.9, 125.2, 125.5, 126.0, 126.3, 128.7, 129.3, 130.2, 134.5, 136.2, 143.0, 147.3, 149.5, 162.3; ESI-HRMS *m/z* calcd for $C_{26}H_{26}ClN_3OS$: 464.15579 $[M+H]^+$, found: 464.15599.

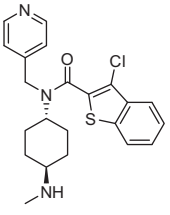

3.1.48. 3-Chloro-*N*-[*trans*-4-(methylamino)cyclohexyl]-*N*-(pyridin-4-ylmethyl)benzo[*b*]-thiophene-2-carboxamide 10m

Light yellow solid, quantitative yield. Mp: 70–72 °C; IR (KBr): $\tilde{\nu}$ = 3290, 2932, 1634, 1599, 1412, 1305, 1244, 756, 727 cm^{-1}; ^{1}H NMR (300 MHz, $(CD_3)_2SO$, 90 °C): δ = 0.86–0.98 (m, 2H), 1.56–1.72 (m, 4H), 1.84–1.88 (m, 2H), 2.21 (s, 3H), 2.25–2.30 (m, 1H), 3.79 (br, 1H), 4.69 (s, 2H), 7.31–7.32 (m, 2H), 7.51–7.60 (m, 2H), 7.84–7.86 (m, 1H), 8.04–8.06 (m, 1H), 8.49–8.51 (m, 2H); ^{13}C NMR (75 MHz, $(CD_3)_2SO$, 90 °C): δ = 28.9, 30.4, 32.3, 44.6 (br), 56.2, 58.0, 117.4, 121.5, 121.6, 122.9, 125.5, 126.4, 130.2, 134.5, 136.2, 147.2, 149.1, 162.3; ESI-HRMS *m/z* calcd for $C_{22}H_{24}ClN_3OS$: 414.14014 $[M+H]^+$, found: 414.14003.

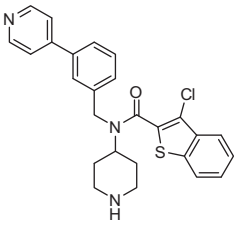

3.1.49. 3-Chloro-*N*-piperidin-4-yl-*N*-(3-pyridin-4-ylbenzyl)benzo[*b*]thiophene-2-carbox- amide 14a

White solid, quantitative yield. Mp: 100–102 °C; IR (KBr): $\tilde{\nu}$ = 3415, 2925, 1633, 1593, 1408, 1285, 1260, 756, 727 cm^{-1}; ^{1}H NMR (400 MHz, $(CD_3)_2SO$, 90 °C): δ = 1.66–1.77 (m, 4H), 2.37–2.39 (m, 2H), 2.96 (br, 2H), 3.98 (br, 1H), 4.81 (s, 2H), 7.44–7.49 (m, 2H), 7.50–7.57 (m, 2H), 7.60–7.61 (m, 2H), 7.65–7.67 (m, 1H), 7.69 (br, 1H), 7.86–7.88 (m, 1H), 8.05–8.08 (m, 1H), 8.64–8.65 (m, 2H); ^{13}C NMR (75 MHz, $(CD_3)_2SO$, 50 °C): δ = 30.3, 42.7, 44.4 (br), 55.4, 117.4, 121.0, 121.8, 123.3, 124.9, 125.0, 125.7, 126.6, 127.3, 129.2, 130.3, 134.6, 136.2, 137.2, 139.3, 146.8, 150.0, 162.6; ESI-HRMS *m/z* calcd for $C_{26}H_{24}ClN_3OS$: 462.14014 $[M+H]^+$, 923.27300 $[2M+H]^+$, found: 462.14025, 923.27265.

3.2. Biological tests

3.2.1. Cell-based assay for Hh pathway activation

Cell assay activation of *Gli1* expression was measured in Shh-Light II cells (ATCC CRL-2795, LGC, Wesel, Germany) as described by Beachy and co-workers[15] Stock solutions of the potential activators of Hh were prepared in DMSO and introduced in different concentration into the culture medium to reach a final solvent concentration of 0.1%. After treatment for 48 h cells were washed with PBS. Harvest and lysis of the cells, measurement of reporter gene and constitutive *Renilla* luminescence were performed with the Dual Luciferase® reporter gene assay system according to the manufacturer's instructions (Promega, Mannheim, Germany). Luminescence was recorded using a GENios reader (TECAN, Crailsheim, Germany). For determination of EC_{50}-values, the relative luminescence units per second RLU/s were plotted against the activator concentrations. Each assay was replicated two to four times (independent experiments) with three technical replicates each.

Analysis of constitutive *Renilla* luminescence was used to normalize for any potential unspecific activation of *Gli1* reporter gene luminescence. Furthermore, microscopic observations of cells did not indicate any toxic effects up to a concentration of 1 μM, the highest concentration tested for all compounds.

3.2.2. Statistical analysis

Concentration-response curves of *Gli1* reporter gene luminescence were fitted with the Hill-slope equation:

$$y = \text{Min} + \frac{\text{Max} - \text{Min}}{1 + (\frac{x}{EC_{50}})^{p}}$$

Data were first normalized so that individual dose-response curves converged to 0 and 100. Subsequently, these normalized data were used to calculate the EC_{50} and corresponding SE and confidence intervals based on 2–4 replicates. Examples for the calculation of concentration-response curves are shown for SAG (**10a**) and **10c**. Calculations were performed using the software jmp (SAS Institute Inc., Cary, NC). EC_{50} with non-overlapping confidence intervals (p <0.05) were considered as significantly different.

3.2.3. Cell viability assay

The cytotoxicity was investigated in human umbilical vein endothelial (HUVE) cells (PromoCell) by incubation with cell proliferation reagent WST-1 (Roche, Mannheim, Germany). Briefly, 7500 cells per well (Greiner Bio-one, 96 well microplate, white, μclear bottom) were exposed to different compound concentrations (100 μl/well, containing less than 0.5% DMSO (v/v)) for 24 h before adding the WST-1 reagent. After 24 h of incubation absorbance (440 nm and 650 nm) was measured according to the test protocol. For determination of cytotoxicity, absorbance difference was plotted against the concentrations of each compound.

3.2.4. Proliferation assay

Cell proliferation was investigated by measuring the incorporation of 5-bromo-2′-deoxyuridine (BrdU, Roche ELISA assay) into HUVE cells (PromoCell). To perform the assay, 5000 cells were seed into each well of a 96 well microplate (Greiner Bio-one, white, μclear bottom) in a final volume of 100 μl per well. After 24 h the medium was replaced and the cells were treated with 100 μl per well of different compound concentrations, so that the DMSO concentration did not exceed 0.5% (v/v). After 48 h of incubation the proliferation status was determined according to the test instructions using an Orion Microplate Luminometer (Bertholt) to measure chemiluminescence.

3.2.5. 3D-Angiogenesis assay (HUVEC)

The ready-to-use 3D-angiogenesis assay (PromoCell, Heidelberg, Germany) utilizes human endothelial cell spheroids (each containing 400–500 cells) embedded in a collagen matrix, which were exposed to different compound concentrations containing less than 0.5% DMSO (v/v) for 48 h. Angiogenic activity was examined according to the manufacturer's instructions using phase-contrast microscope and ImageJ software.

3.2.6. ELISA

Primary fibroblasts of foreskin tissue were placed on plastic culture dishes in Dulbecco's modified Eagle's medium (Gibco) containing 10% fetal bovine serum (FBS) for 24 h. After removing of nonadherent cells by washing with PBS (Gibco) cells were reseed on 24 well plates (14000 cells per well) in a final volume of 500 μl per well. After 72 h the medium was replaced and the cells were treated by different compound concentration (500 μl per well, containing less than 0.1% DMSO (v/v)). After incubation for 48 h at 37 °C and 5% CO_2 cell supernatants were taken and stored at −20 °C.

$VEGF_{165}$-concentration in conditioned media from compound-treated cells was compared with vehicle-treated cells. $VEGF_{165}$ was determined per manufacturer's instructions using the Quantikine human VEGF-ELISA kit (R&D Systems, Wiesbaden, Germany). The concentrations were determined using a 96 well ELISA plate reader (Tecan, Salzburg, Austria) and Magellan standard software. Each assay was replicated three times by independent experiments.

Acknowledgments

We thank Dr. Stefan Scholz (UFZ-Helmholtz Centre for Environmental Research, Department of Bioanalytical Ecotoxicology, Leipzig) for the ability to conduct the cell-based assay for Hh pathway activation in his facilities, and Dr. Lothar Hennig for recording NMR spectra. This work was partly financially supported by the TRM-Translational Centre of Regenerative Medicine Leipzig.

Supplementary data

Supplementary data associated with this article can be found, in the online version, at http://dx.doi.org/10.1016/j.bmc.2012.08.026.

References and notes

1. (a) Chiang, C.; Litingtung, Y.; Lee, E., et al *Nature* **1996**, *383*, 407; (b) Pepicelli, C. V.; Lewis, P. M.; McMahon, A. P. *Curr. Biol.* **1998**, *8*, 1083; (c) Ramalho-Santos, M.; Melton, D. A.; McMahon, A. P. *Development* **2000**, *127*, 2763; (d) Taipale, J.; Beachy, P. A. *Nature* **2001**, *411*, 349.
2. (a) Beachy, P. A.; Karhadkar, S. S.; Berman, D. M. *Nature* **2004**, *432*, 324; (b) Zhao, C.; Chen, A.; Jamieson, C. H.; Fereshteh, M.; Abrahamsson, A.; Blum, J.; Kwon, H. Y.; Kim, J.; Chute, J. P.; Rizzeri, D.; Munchhof, M.; Van Arsdale, T.; Beachy, P. A.; Reya, T. *Nature* **2009**, *458*, 776; (c) Lavine, K. J.; Long, F.; Choi, K.; Smith, C.; Ornitz, D. M. *Development* **2008**, *135*, 3161.
3. Ingham, P. W.; McMahon, A. P. *Genes Dev.* **2001**, *15*, 3059.
4. (a) Porter, J. A.; Young, K. E.; Beachy, P. A. *Science* **1996**, *274*, 255; (b) Chamoun, Z.; Mann, R. K.; Nellen, D.; Kessler, D. P.; Bellotto, M.; Beachy, P. A.; Basler, K. *Science* **2001**, *293*, 2080; (c) Ingham, P. W. *Science* **2001**, *294*, 1879.
5. Aikin, R. A.; Ayers, K. L.; Therond, P. P. *EMBO Rep.* **2008**, *9*, 330.
6. (a) Huangfu, D.; Anderson, K. V. *Proc. Natl. Acad. Sci. U.S.A.* **2005**, *102*, 11325; (b) Rohatgi, R.; Milenkovic, L.; Scott, M. P. *Science* **2007**, *317*, 372; (c) Wang, Y.; Zhou, Z.; Walsh, C. T.; McMahon, A. P. *Proc. Natl. Acad. Sci. U.S.A.* **2009**, *106*, 2623.
7. McMahon, A. P.; Ingham, P. W.; Tabin, C. J. *Curr. Top. Dev. Biol.* **2003**, *53*, 1.
8. (a) Sato, N.; Leopold, P. L.; Crystal, R. G. *J. Clin. Invest.* **1999**, *104*, 855; (b) Reddy, S.; Andl, T.; Bagasra, A.; Lu, M. M.; Epstein, D. J.; Morrisey, E. E.; Millar, S. E. *Mech. Dev.* **2001**, *107*, 69.
9. (a) Levy, V.; Lindon, C.; Zheng, Y.; Harfe, B. D.; Morgan, B. A. *FASEB J.* **2007**, *21*, 1358; (b) Ito, M.; Yang, Z.; Andl, T.; Cui, C.; Kim, N.; Millar, S. E.; Cotsarelis, G. *Nature* **2007**, *447*, 316.
10. Pola, R.; Ling, L. E.; Silver, M.; Corbley, M. J.; Kearney, M.; Pepinsky, R. B.; Shapiro, R.; Taylor, F. R.; Baker, D. P.; Asahara, T.; Isner, J. M. *Nat. Med.* **2001**, *7*, 706.
11. Kanda, S.; Mochizuki, Y.; Suematsu, T.; Miyata, Y.; Nomata, K.; Kanetake, H. *J. Biol. Chem.* **2003**, *278*, 8244.
12. Asai, J.; Takenaka, H.; Kusano, K. F.; Ii, M.; Luedemann, C.; Curry, C.; Eaton, E.; Iwakura, A.; Tsutsumi, Y.; Hamada, H.; Kishimoto, S.; Throne, T.; Kishore, R.; Losordo, D. W. *Circulation* **2006**, *113*, 2413.
13. Emanueli, C.; Madeddu, P. *Br. J. Pharmacol.* **2001**, *133*, 951.
14. Chinchilla, P.; Xiao, L.; Kazanietz, M. G.; Riobo, N. A. *Cell Cycle* **2010**, *9*, 570.
15. Chen, J. K.; Talpale, J.; Young, K. E.; Maltl, T.; Beachy, P. A. *Proc. Natl. Acad. Sci. U.S.A.* **2002**, *99*, 14071.
16. (a) Wu, X.; Walker, J.; Zhang, J.; Ding, S.; Schultz, P. G. *Chem. Biol.* **2004**, *11*, 1229; (b) Sinha, S.; Chen, J. K. *Nat. Chem. Biol.* **2006**, *2*, 29.
17. Ducruet, A. P.; Rice, R. L.; Tamura, K.; Yokokawa, F.; Yokokwara, S.; Wipf, P.; Lazo, J. S. *Bioorg. Med. Chem.* **2000**, *8*, 1451.
18. Wang, N.; Xiang, J.; Ma, Z.; Quan, J.; Chen, J.; Yang, Z. *J. Comb. Chem.* **2008**, *10*, 825.
19. Frank-Kamenetsky, M.; Zhang, X. M.; Bottega, S.; Guicherit, O.; Wichterle, H.; Dudek, H.; Bumcrot, D.; Wang, F. Y.; Jondes, S.; Shulok, J.; Rubin, L. L.; Porter, J. A. *J. Biol.* **2002**, *1*, 10.
20. Baxter, A.D.; Boyd, E.A.; Guicherit, O.M.; Porter, J.; Price, S.; Rubin, L.E. *PCT Int. Appl.*, **2001**; WO 2001074344 A2 20011011.
21. Brunton, S. A.; Stibbard, J. H.; Rubin, L. L.; Guicherit, O. M.; Kruse, L. I.; Price, S.; di Lucrezia, R.; MacKinnon, C. H.; Avery, A.; Park, Y.; Buxton, D.; Boyd, E. A. *Bioorg. Med. Chem. Lett.* **2009**, *19*, 4308.
22. Büttner, A.; Seifert, K.; Cottin, T.; Sarli, V.; Tzagkaroulaki, L.; Scholz, S.; Giannis, A. *Bioorg. Med. Chem.* **2009**, *17*, 4943.
23. Jenkins, D. *Cell. Signalling* **2009**, *21*, 1023.